

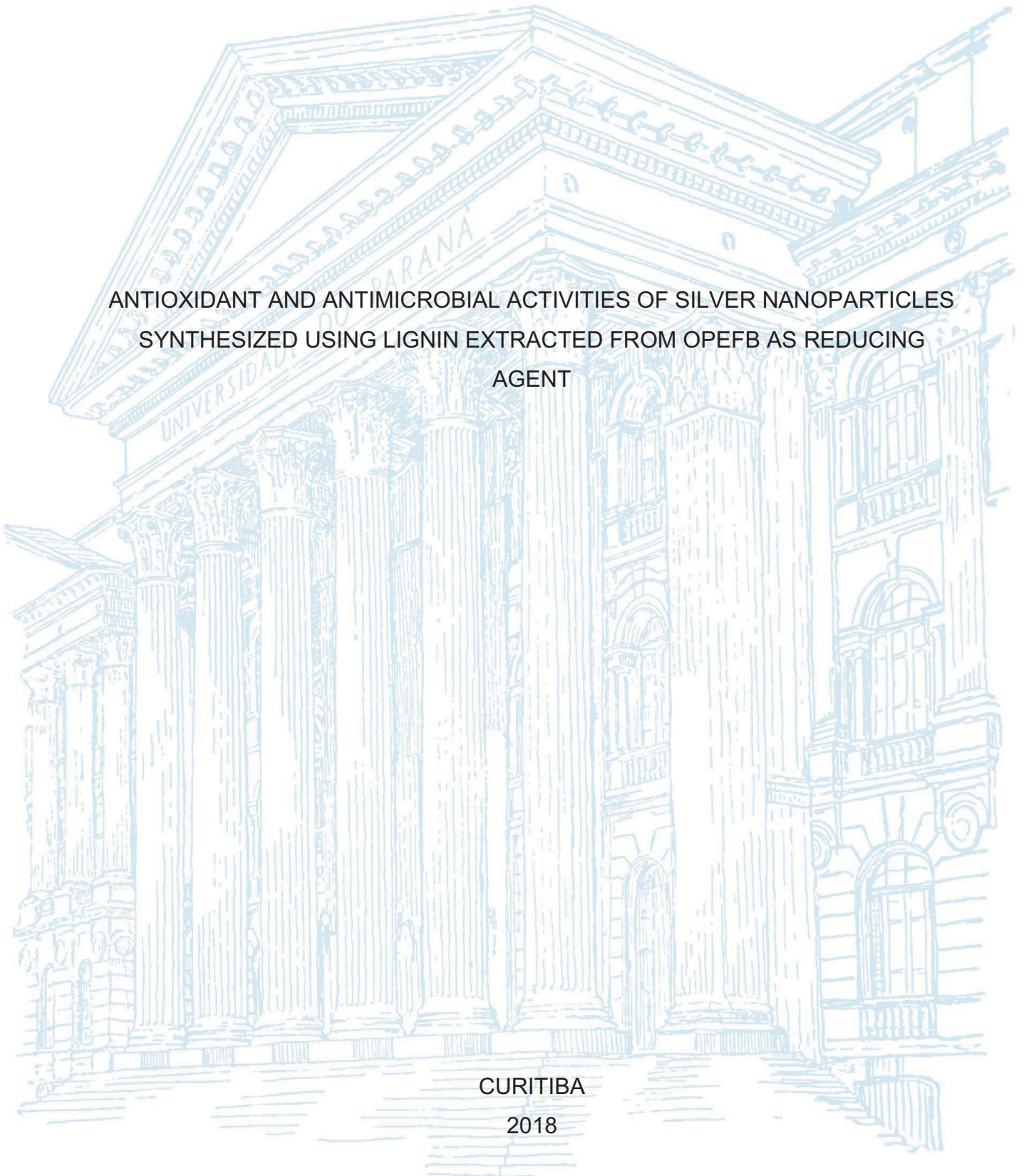
UNIVERSIDADE FEDERAL DO PARANÁ

LUIS ALBERTO ZEVALLOS TORRES

ANTIOXIDANT AND ANTIMICROBIAL ACTIVITIES OF SILVER NANOPARTICLES
SYNTHESIZED USING LIGNIN EXTRACTED FROM OPEFB AS REDUCING
AGENT

CURITIBA

2018



LUIS ALBERTO ZEVALLOS TORRES

ANTIOXIDANT AND ANTIMICROBIAL ACTIVITIES OF SILVER NANOPARTICLES
SYNTHESIZED USING LIGNIN EXTRACTED FROM OPEFB AS REDUCING
AGENT

Dissertação apresentada ao curso de Pós-Graduação em Engenharia de Bioprocessos e Biotecnologia, Setor de Tecnologia, Universidade Federal do Paraná, como requisito parcial à obtenção do título de Mestre em Engenharia de Bioprocessos e Biotecnologia.

Orientadora: Profa. Dra. Adenise Lorenci Woiciechowski

Coorientadora: Dra. Valcineide Oliveira de Andrade Tanobe

CURITIBA

2018

Catálogo na Fonte: Sistema de Bibliotecas, UFPR
Biblioteca de Ciência e Tecnologia

T693a

Torres, Luis Alberto Zevallos

Antioxidant and antimicrobial activities of silver nanoparticles synthesized using lignin extracted from OPEFB as reducing agent / Luis Alberto Zevallos Torres. – Curitiba, 2018.

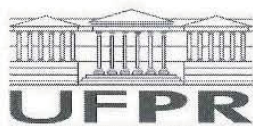
Dissertação - Universidade Federal do Paraná, Setor de Tecnologia, Programa de Pós-Graduação em Engenharia de Bioprocessos e Biotecnologia, 2018.

Orientador: Adenise Lorenci Woiciechowski – Coorientador: Valcineide Oliveira de Andrade Tanobe.

1. Lignina. 2. Nanopartículas. 3. Óleo de palma. 4. Antioxidantes. 5. Testes de sensibilidade bacteriana. I. Universidade Federal do Paraná. II. Woiciechowski, Adenise Lorenci. III. Tanobe, Valcineide Oliveira de Andrade. IV. Título.

CDD: 662.88

Bibliotecário: Elias Barbosa da Silva CRB-9/1894



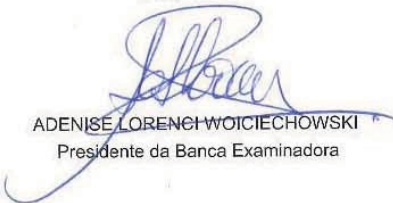
MINISTÉRIO DA EDUCAÇÃO
SETOR TECNOLOGIA
UNIVERSIDADE FEDERAL DO PARANÁ
PRÓ-REITORIA DE PESQUISA E PÓS-GRADUAÇÃO
PROGRAMA DE PÓS-GRADUAÇÃO ENGENHARIA DE
BIOPROCESSOS E BIOTECNOLOGIA

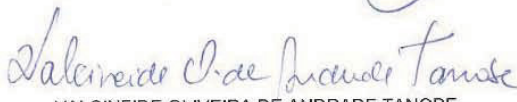
TERMO DE APROVAÇÃO

Os membros da Banca Examinadora designada pelo Colegiado do Programa de Pós-Graduação em ENGENHARIA DE BIOPROCESSOS E BIOTECNOLOGIA da Universidade Federal do Paraná foram convocados para realizar a arguição da Dissertação de Mestrado de **LUIS ALBERTO ZEVALLOS TORRES** intitulada: **Antioxidant and antimicrobial activities of silver nanoparticles synthesized using lignin extracted from OPEFB as reducing agent**, após terem inquirido o aluno e realizado a avaliação do trabalho, são de parecer pela sua aprovação no rito de defesa.

A outorga do título de mestre está sujeita à homologação pelo colegiado, ao atendimento de todas as indicações e correções solicitadas pela banca e ao pleno atendimento das demandas regimentais do Programa de Pós-Graduação.

Curitiba, 06 de Outubro de 2017.


ADENISE LORENCI WOICIECHOWSKI
Presidente da Banca Examinadora


VALCINEIDE OLIVEIRA DE ANDRADE TANOBE
Avaliador Externo


CRAIG FAULDS
Avaliador Externo


CARLOS RICARDO SOCCOL
Avaliador Interno


LAURENCE LESAGE-MEESSEN
Avaliador Externo

Os Avaliadores Externos Laurence Lesage-Meesen e Craig Faulds participaram por videoconferência - Ata homologada na 67ª Reunião de Colegiado realizada no dia 09 de novembro de 2017.

AGRADECIMENTOS

À Deus pela vida e suporte durante cada momento no desenvolvimento do presente trabalho.

À minha orientadora, Profa. Dra. Adenise Lorenci Woiciechowski, por acompanhar todo o trabalho, pela ajuda, recomendações e sugestões.

À o Prof. Dr. Carlos Ricardo Soccol pelo apoio e oportunidade brindada de ser parte do PPGEBB.

À Dra. Valcineide Oliveira de Andrade Tanobe pela ajuda, suporte, recomendações e artigos compartilhados durante todo o processo de experimentação e análises.

À o Prof. Dr. Rilton Alves de Freitas por esclarecer as minhas dúvidas e ajudar na interpretação de resultados do Potencial Zeta e DLS.

À o Prof. Dr. Miguel Nosedá pela ajuda e suporte nas análises de RMN.

À Mitiyo Miyaoka pela paciência no ensino das técnicas de microbiologia básica e as minhas primeiras experiências com os microrganismos.

À todos os bons amigos que eu fiz no Brasil, no laboratório, com os quais compartilhamos muitas horas de estudo, metodologias, brincadeiras, tristezas e risadas: Andrés Camargo, Cristina Ferrer, Denisse Molina, Emerson Ortega, Marcelino Xavier e por último mas não menos importante, Walter Burgos.

À os meus pais Lucía e Alberto os quais estando muito longe eu sentia eles sempre perto de mim dando-me suporte e conselho.

À todas as pessoas que eu conheci durante a minha experiência no laboratório.

À todos aqueles que contribuíram direta e indiretamente no presente trabalho.

RESUMO

As ligninas extraídas dos OPEFB a quatro condições diferentes foram utilizadas na síntese de nanopartículas de prata. Os espectros UV-vis apresentam os picos SPR à 423-427 nm. As análises MET mostram as nanopartículas de forma esférica e de natureza policristalina. Os espectros FT-IR das AgNPs apresentam grupos funcionais correspondentes às ligninas utilizadas como agente redutor e de recobrimento. O tamanho médio de partícula das AgNPs esteve na faixa de 17,63 até 19,24 nm. Um perfil de potencial Zeta negativo para as AgNPs foi observado em meio com baixa concentração de íons. A atividade antioxidante das AgNPs poderia ser atribuída à lignina utilizada na síntese. As atividades antimicrobianas de todas as AgNPs foram testadas contra *Escherichia coli* e a CMI para a HAL3-L AgNP foi de 62,5 ug.mL⁻¹.

Palavras-chave: Lignina. Nanopartículas de prata. Oil Palm Empty Fruit Bunches. Atividade antioxidante. Atividade antimicrobiana.

ABSTRACT

Lignins extracted from OPEFB at four different conditions were used for synthesis of silver nanoparticles. UV–vis spectra show the SPR peak at 423–427 nm. TEM analysis exposes the spherical shape and polycrystalline nature of nanoparticles. FT-IR spectra of AgNPs show the presence of functional groups corresponding to the lignins used as reducing and capping agents. The average particle size of AgNPs ranged from 17.63 to 19.24 nm. A negative Zeta potential profile for AgNPs suspensions was exhibited in a low ion concentration medium. Antioxidant activity of AgNPs could be attributed to the lignin used in the synthesis. The antibacterial activity of all AgNPs was demonstrated against *Escherichia coli* and the MIC for HAL3-L AgNP was 62.5 $\mu\text{g}\cdot\text{mL}^{-1}$.

Keywords: Lignin. Silver nanoparticles. Oil palm empty fruit bunches. Antioxidant activity. Antimicrobial activity.

LISTA DE FIGURAS

FIGURE 1 - 2D HSQC SPECTRA OF DIFFERENT LIGNIN SAMPLES: (a) HAL1-L; (b) HAL2-L; (c) HAL3-L; AND (d) HAL4-L. SOLVENT d6-DMSO. TEMPERATURE 30°C	27
FIGURE 2 - MAIN STRUCTURES PRESENT IN OPEFB LIGNIN: (A) β -O-4' ARYL ETHER LINKAGES; (S) SYRINGYL UNITS AND (G) GUAIACYL UNITS	28
FIGURE 3 - VISUAL OBSERVATION AND UV-VISIBLE SPECTRA OF REACTION MIXTURES (TUBE A) USING DIFFERENT LIGNINS (TUBE B): (a) HAL1-L, (b) HAL2-L, (c) HAL3-L AND (d) HAL4-L. (e) COMPARISON OF SURFACE PLASMON RESONANCE PEAKS OF AGNPS USING FOUR DIFFERENT LIGNINS.....	31
FIGURE 4 - BRIGHT FIELD TEM, DARK FIELD TEM AND SAED PATTERN SHOWING DIFFERENT CRYSTALLINE PATTERNS OF AgNPS SYNTHESIZED USING DIFFERENT LIGNINS	33
FIGURE 5 - FT-IR SPECTRA OF (a) LIGNINS AND (b) SILVER NANOPARTICLES SYNTHESIZED WITH DIFFERENT LIGNINS.....	34
FIGURE 6 - AVERAGE PARTICLE SIZE DISTRIBUTION OF AGNPS USING DIFFERENT LIGNINS AS REDUCING AGENT: HAL1-L, HAL2-L, HAL3-L AND HAL4-L.	36
FIGURA 7 - ZETA POTENTIAL AS A FUNCTION OF pH FOR AgNPS SYNTHESIZED USING DIFFERENT LIGNINS: HAL1-L, HAL2-L, HAL3-L, HAL4-L. A) AGNPS DISSOLVED IN ULTRAPURE WATER AND B) IN MUELLER-HINTON BROTH	38
FIGURA 8 - ANTIOXIDANT ACTIVITY (DPPH): (A) SCAVENGING ACTIVITY OF LIGNINS AT DIFFERENT CONCENTRATIONS (200, 100, 50 AND 25 $\mu\text{g}.\text{mL}^{-1}$); (B) INHIBITORY CONCENTRATION OF 50% OF FREE-RADICAL BY DIFFERENT LIGNINS; (C) SCAVENGING ACTIVITY OF RESULTING SOLUTIONS FROM THE SYNTHESIS OF AgNPS DIFFERENT CONCENTRATIONS (100, 50, 25 AND 12.5%).....	40
FIGURA 9 - ANTIMICROBIAL ACTIVITY – DISK DIFFUSION METHOD COMPARING THE RESULTING SOLUTIONS OF SILVER	

NANOPARTICLES SYNTHESIZED WITH DIFFERENT LIGNINS:	
HAL1-L, HAL2-L, HAL3-L AND HAL4-L	41

LISTA DE TABELAS

TABLE 1 – OPEFB ACID HYDROLYSIS CONDITIONS	21
TABLE 2 – ASSIGNMENTS OF ¹³ C- ¹ H CORRELATION SIGNALS IN THE 2D HSQC NMR SPECTRA CORRESPONDING TO EACH NON-ACETYLATED LIGNIN SAMPLE.....	28
TABLE 3 – SURFACE PLASMON RESONANCE OF AgNPS USING FOUR DIFFERENT LIGNINS.....	32
TABLE 4 – LATTICE SPACING (<i>d</i>) OF AgNPS SYNTHESIZED WITH DIFFERENT LIGNINS.....	34
TABLE 5 – FT-IR STRETCHING FREQUENCIES FOUND ON LIGNINS AND CORRESPONDING AgNPS	35
TABLE 6 – AVERAGE PARTICLE SIZE OF AgNPS SYNTHESIZED WITH DIFFERENT LIGNINS.....	36
TABLE 7 – INHIBITION ZONES DEVELOPED BY DIFFERENT AgNPS AGAINST <i>Escherichia coli</i> ATCC 35218.....	41

LISTA DE ABREVIATURAS OU SIGLAS

AgNPs	- Silver nanoparticles
DLS	- Dynamic light scattering
EFB	- Empty fruit bunches
FFB	- Fresh fruit bunches
FT-IR	- Fourier-Transformed Infrared
GPC	- Gel Permeation Chromatography
HSQC	- Heteronuclear Single Quantum Correlation
MIC	- Minimum inhibitory concentration
NMR	- Nuclear Magnetic Resonance
OPEFB	- Oil palm empty fruit bunches
Py-GC/MS	- Pyrolysis Gas Chromatography Mass Spectrometry
SAED	- Selected Area Electron Diffraction
SPR	- Surface Plasmon Resonance
TEM	- Transmission electron microscopy

SUMÁRIO

1 INTRODUCTION	16
1.1 OBJECTIVES	16
1.1.1 General objectives.....	16
1.1.2 Specific objectives.....	16
2 BIBLIOGRAPHIC REVIEW	18
2.1 NANOPARTICLES.....	18
2.2 SILVER NANOPARTICLES	18
2.3 LIGNIN EXTRACTED FROM OIL PALM EMPTY FRUIT BUNCHES USED AS REDUCING AGENT	19
3 MATERIALS AND METHODS	21
3.1 LIGNIN EXTRACTION FROM OIL PALM EMPTY FRUIT BUNCHES.....	21
3.2 SYNTHESIS OF SILVER NANOPARTICLES	22
3.3 CHARACTERIZATION	22
3.3.1 NUCLEAR MAGNETIC RESONANCE (NMR)	22
3.3.2 UV–VIS ABSORBANCE SPECTROSCOPY ANALYSIS.....	23
3.3.3 TRANSMISSION ELECTRON MICROSCOPY (TEM) ANALYSIS OF NANOPARTICLES	23
3.3.4 FOURIER-TRANSFORMED INFRARED (FT-IR) SPECTROSCOPY ANALYSIS 23	
3.3.5 DYNAMIC LIGHT SCATTERING (DLS) AND ZETA POTENTIAL OF NANOPARTICLES	24
3.3.6 ANTIOXIDANT ACTIVITY	24
3.3.7 ANTIMICROBIAL ACTIVITY	24
3.3.7.1 DISK DIFFUSION TEST.....	25
3.3.7.2 MINIMUM INHIBITORY CONCENTRATION (MIC).....	25
4 RESULTS AND DISCUSSION	26
4.1 2D HSQC NMR CHARACTERIZATION.....	26
4.2 VISUAL OBSERVATIONS AND UV-VISIBLE SPECTROSCOPY	29
4.3 TRANSMISSION ELECTRON MICROSCOPY (TEM) ANALYSIS.....	33
4.4 FOURIER-TRANSFORMED INFRARED (FT-IR) SPECTROSCOPY ANALYSIS 34	
4.5 PARTICLE SIZE DISTRIBUTION.....	36

4.6 ZETA POTENTIAL	37
4.7 ANTIOXIDANT ACTIVITY (DPPH).....	39
4.8 ANTIMICROBIAL ACTIVITY	41
5 CONCLUSIONS.....	44
REFERENCES.....	45

1 INTRODUCTION

Plant biomass is the most abundant renewable biomass on earth and it is considered as an attractive source of bioenergy and biobased chemicals (Gonzalo et al. 2016). It is mainly composed of lignin, cellulose and hemicellulose where lignin constitutes up to one-third of the material found in plant cell walls and it is the second most abundant natural polymer in the world (Eudes et al. 2014; Brenelli et al. 2016). Compared to other bio-polymers such as starch, cellulose, hemicelluloses, etc. lignin is a very intricate molecule since its structure and bonding between various units varies according to plant species, age of plant, type of plant, growing conditions (temperature, humidity, soil quality, time, etc.) and most importantly isolation procedure employed for its extraction (Singh and Dhepe 2016). Lignin acts as a structural material that adds strength and rigidity to the plant cell walls and constitutes between 15% and 40% of the dry matter of woody plants and from 12 to 21% of dry matter in main straw species (Doherty et al. 2011a; Ghaffar and Fan 2014). Refer to table 1 for some examples about the lignin content in different lignocellulosic biomass. In terms of production, by the first half of previous century, lignin was already considered as the major industrial by-product (Gottlieb and Pelczar 1951). By 2010, the pulp and paper industry alone was estimated to produce lignin as a residue in amounts near to 50 million tons per year, which were used primarily for energy generation and only about 1-2% was used for manufacturing low-value specialty products such as dispersing or binding agents (Lora and Glasser 2002; Higson and Smith 2011; Smolarski 2012). The aim of this work is to give value to lignin in the production of silver nanoparticles.

1.1 OBJECTIVES

1.1.1 General objectives

To produce silver nanoparticles using lignin extracted from oil palm empty fruit bunches as reducing and stabilizing agent.

1.1.2 Specific objectives

To extract lignin from oil palm empty fruit bunches (OPEFB) at four different conditions of acid hydrolysis.

To characterize the lignin extracted from OPEFB.

To synthesize the silver nanoparticles using each the lignin extracted from OPEFB.

To characterize the silver nanoparticles (AgNPs).

To test the antioxidant and antimicrobial activity of extracted lignins and AgNPs.

2 BIBLIOGRAPHIC REVIEW

2.1 NANOPARTICLES

Nanoparticles, having a diameter smaller than 100 nm, are defined as ultrafine particles exhibiting unique size- and shape-dependent properties Manikprabhu; Lingappa (2014 e Singh et al. (2016). The synthesis of metal nanoparticles and nanostructured materials is attracting attention in recent research because of their valuable properties which make them useful in many applications such as catalysis Wang et al. (2014), sensor technology Tagad et al. (2013), food industry Azeredo et al. (2015), electronics, drug delivery Prow et al. (2011), and biomedical applications Ali et al. (2016). The synthesis of metal nanoparticles can be made using various methods, including chemical and physical methods Ghoreishi et al. (2011 e Suman et al. (2013). Although most of these may successfully produce pure and well-defined nanoparticles, their main disadvantages remain on the use of extremely expensive processes which require high energy consumption and the toxic and hazardous chemicals used that could remain adsorbed on the surface, leading to adverse effects in its application Amooaghaie et al. (2015 e Wei et al. (2015). An alternative to traditional methods in an eco-friendly and safer manner we find the “biological” or “green” synthesis methods which usually involve the use of microorganisms, plant extracts or natural compounds to bioreduce metal ions Narayanan; Sakthivel (2011). It must be stated that using plant extracts is potentially advantageous over microorganisms due to the ease of biohazards and the culture of the microorganisms Zhang et al. (2013).

2.2 SILVER NANOPARTICLES

Among the various metal nanoparticles, silver nanoparticles (AgNP) are new kind of nano-materials in further study and expands rapidly, since the obtained nanoparticles possess unique electrical, optical Kurihara et al. (2005), catalytic Bindhu; Umadevi (2015), sensing Shen et al. (2016), as well as antimicrobial properties Rao et al. (2016). Several decades ago, the AgNP synthesis was done by traditional chemical and physical methods. Subsequently, researchers opted the synthesis by using green methods which involve the use of microbes such as bacteria Nanda; Saravanan (2009), El-Rafie et al. (2013) and fungi Sanghi; Verma (2009). Both intra and extracellular methods are used for the AgNP synthesis from which the extracellular

method is mostly preferred due to its simplicity, large-scale synthesis and easier downstream processing Jeyaraj et al. (2013). On the other hand, natural products and plant extracts such as essential oils Vilas et al. (2016), caffeic acid Guo et al. (2015), polyhydroxyalkanoates Castro-Mayorga et al. (2014), *Malus domestica* extract Lokina et al. (2014), *Rosmarinus officinalis* leaves extract Ghaedi et al. (2015), *Typha angustifolia* leaves extract Gurunathan (2015), *Allium cepa* extract Khalilzadeh; Borzoo (2016), and even plant latex from *Euphorbia nivulia* Valodkar et al. (2011) have been reported as reducing agents for the production of silver nanoparticles.

2.3 LIGNIN EXTRACTED FROM OIL PALM EMPTY FRUIT BUNCHES USED AS REDUCING AGENT

Oil palm (*Elaeis guineensis*) is grown as a plantation crop in most countries with high rainfall in tropical climates, principally for processing the palm fruits in order to obtain edible and technical oils. Being Indonesia and Malaysia the two major producers with around 85% of the world palm oil production, Brazil represents the third producer in South America with a production of 410000 metric tons (0.62% of the world production) [Www.indexmundi.com](http://www.indexmundi.com) (2017). It is estimated that approximately 100 tons of fresh fruit bunches (FFB) can generate 20-22 tons of empty fruit bunches (EFB) which are mainly composed by 30.5% cellulose, 19.5% hemicellulose and 32.17% acid insoluble lignin Coral Medina et al. (2015 e Hosseini; Wahid (2014). The oil palm empty fruit bunches (OPEFB), like any other plant biomass are mainly composed of lignin, cellulose and hemicellulose where lignin constitutes up to one-third of the material found in plant cell wall and it is the second most abundant natural polymer. Compared to other bio-polymers such as starch, cellulose, hemicelluloses, etc. lignin is a very intricate molecule since its structure and bonding between various units varies according to plant species, age of plant, type of plant, growing conditions (temperature, humidity, soil quality, time, etc.) and most importantly isolation procedure employed for its extraction Singh; Dhepe (2016). Lignin is a three-dimensional amorphous macromolecule composed by crosslinked phenylpropanoid structures of sinapyl, coniferyl and p-coumaryl alcohols which give rise to the syringyl (S), guaiacyl (G) and p-hydroxyphenyl (H) lignin units, respectively Boerjan et al. (2003 e Tejado et al. (2007). Most softwood lignins consist predominantly of G units, whereas hardwood and herbaceous (grass/straw) lignins contain G, S and H in different ratios Boeriu et al. (2014 e Capanema et al. (2005 e Obst (1982). Due to the presence of reducing

functional groups in its structure, lignin has a potential for being used as reducing agent of metal ions like silver Aadil et al. (2014 e Hu; Hsieh (2016) In consequence, lignin extracted from OPEFB which has shown a relatively high redox potential Coral Medina et al. (2016) possess the capacity of bioreducing silver ions. Hu; Hsieh (2016) reported the use of the commercial Alkali lignin (Sigma-Aldrich) as reducing agent in the synthesis of AgNPs to study the kinetics and reaction mechanism. Furthermore, Milczarek et al. (2013) used another commercial sodium softwood lignosulfonate (SLS) (Borregaard LignoTech) as reducing agent for the production of AgNPs with formation of a $\text{Ag}[\text{NH}_3]_2^+$ complex by addition of ammonia in the AgNO_3 solution to ensure a slow reaction between SLS and Ag^+ that would lead to a smaller particle size of reduced silver. Additionally, Aadil et al. (2016) developed a single step procedure for the AgNPS synthesis using lignin extracted from Acacia wood powder as reducing and capping agent with application on hydrogen peroxide sensing.

In the present work, oil palm empty fruit bunches (OPEFB) were used as a source of lignin after being submitted to a sequential acid/alkaline treatment at different conditions, presenting the possibility to take advantage of the hemicellulose, cellulose and lignin fractions from this biomass. Subsequently, a green protocol was described using the different lignin samples obtained as both reducing and stabilizing agent of silver nanoparticles. This synthesis was carried out without any other surfactant or capping agent. The nanoparticles were characterized by UV-visible spectroscopy, FT-IR spectroscopy, dynamic light scattering (DLS), Zeta potential and transmission electron microscopy (TEM) analysis. The application of these green synthesized nanoparticles as antioxidant and antimicrobial agents was also discussed.

3 MATERIALS AND METHODS

Silver nitrate was obtained from Cennabras-Brasil (purity 99.80%). Solvents like methanol were purchased from Alphatec-Brasil. Other reagents like 2,2-Diphenyl-1-picrylhydrazyl (DPPH), rezasurin were purchased from Sigma-Aldrich. All glassware used was overnight soaked in 10% (v/v) nitric acid, rinsed in deionized water 3 times and finally dried in oven before use. Oil palm empty fruit bunches (OPEFB) were obtained from Biopalm Vale factory, located in Mojú, in the state of Pará, Brazil. The OPEFB used for all experiments was dried in an air-circulating oven at 65°C for 48 h. The dried OPEFB were then milled in a hammer mill (Marconi, MA580/E) and the particle size used was the portion that passed through an ASTM No. 20 (0.85 mm) and not through a ASTM No. 45 (0.35 mm) sieve.

3.1 LIGNIN EXTRACTION FROM OIL PALM EMPTY FRUIT BUNCHES

The lignin samples were obtained from OPEFB using sequential acid-alkaline pretreatment. First, the dried lignocellulosic material was submitted to a dilute acid hydrolysis at the conditions detailed on table 1.

TABLE 1 – OPEFB ACID HYDROLYSIS CONDITIONS

Acid hydrolysis Condition	Acid type	Acid concentration (% wt.)	Time (min)	Temperature (°C)
HAL1	HCl	1.5	20	130
HAL2	HCl	3.5	60	130
HAL3	H ₂ SO ₄	1.5	20	130
HAL4	H ₂ SO ₄	3.5	60	130

SOURCE: The author (2017).

For the acid hydrolysis, a solid-liquid relation of 10% wt. was maintained for all the experiments. The resulting products of the acid hydrolysis were filtered using Whatman filter paper No. 40 and washed twice with deionized water to remove excess of acid and carbohydrates. The solid material that remained on the filter paper was dried in a cross flow stove at 45°C for 24 h. Subsequently, the dried solid material obtained from the acid hydrolysis was further submitted to the alkaline extraction process. The mass percentage of NaOH was fixed to 2.5% wt., the mass percentage of biomass was 10% wt. and the process was developed in an autoclave at 121°C for 60 minutes. After the alkaline extraction process, the liquid fraction which contained

the extracted lignin was acidified with 10% wt. H₂SO₄ until achieving pH equal to 2. The precipitated lignin was filtered using Whatman filter paper No. 40 and washed three times with hot deionized water at 70°C to remove the residual sugars. Finally, the washed lignin was vacuum dried at 50°C for 8 h. For all the experiments where the lignin samples were used in a solubilized form, the dried lignin samples were solubilized in alkaline water at pH 11 using a magnetic stirrer at 80°C. After complete solubilization of lignin, the pH of the resulting solution was adjusted to 6-7 using 2% wt. H₂SO₄.

3.2 SYNTHESIS OF SILVER NANOPARTICLES

The synthesis of the silver nanoparticles was carried out as follows. An aqueous solution of lignin at a concentration of 200 µg.mL⁻¹ was prepared as described lines above (solution I). Separately, an aqueous solution of 20 mM AgNO₃ was prepared by dissolving the necessary amount of the silver salt in deionized water (solution II). Then, from each solution (I and II) a certain volume was taken so that the final concentrations of lignin and silver nitrate in the reaction mixture were finally 40 µg.mL⁻¹ and 2 mM, respectively. The reaction took place at 80°C for 4.5 hours without mixing or shaking and covered from the light Hu; Hsieh (2016). A control containing only lignin and silver nitrate solutions separately were also performed. After the reaction took place, the resulting solutions of nanoparticles (hybrid lignin/AgNP, as unreacted bulk reagents were not removed) were submitted to analysis UV-visible spectroscopy, Dynamic Light Scattering (DLS) and Zeta Potential. For other analysis, the resulting solutions of nanoparticles were dried at 45°C. The dried powders were characterized by Transmission Electron Microscope (TEM) and Fourier Transform Infrared Radiation (FTIR).

3.3 CHARACTERIZATION

3.3.1 NUCLEAR MAGNETIC RESONANCE (NMR)

The ¹³C NMR spectra were recorded using a Bruker spectrometer at 400 MHz. About 40 mg of lignin was dissolved in 0.5 mL of dimethylsulfoxide (DMSO-d₆). The chemical shift for ¹³C NMR was calibrated with reference to DMSO-d₆, which standard peak was found at 39.51 ppm. The spectra were recorded for all the samples keeping the following parameters constant: an acquisition time of 0.68 s, frequency of 125 MHz, receiver gain of 203, spectral width of 24038.46 Hz and temperature of 30°C.

The ^1H NMR analysis were conducted in the same equipment described earlier. About 20 mg of lignin samples were dissolved in 0.5 mL of DMSO- d_6 . The chemical shifts of ^1H NMR spectra were calibrated with reference to DMSO- d_6 standard peak at 2.50 ppm. The acquisition parameters used were: acquisition time of 7.69 s, frequency of 125 MHz, receiver gain of 40.3, spectral width of 4261.36 Hz and temperature of 30°C.

The samples submitted to ^1H NMR analysis were also used for 2D HSQC NMR (Two dimensional Heteronuclear Single Quantum Correlation - Nuclear Magnetic Resonance) analysis. The acquisition time were 0.24 and 0.002 s for the ^1H and ^{13}C dimensions, respectively. The spectral width were 4261.36 and 22137.02 Hz for the ^1H and ^{13}C dimensions, respectively. The filter width was 125 MHz, the receiver gain was 203 and the analysis temperature 30°C.

3.3.2 UV–VIS ABSORBANCE SPECTROSCOPY ANALYSIS

The bioreduction of the Ag^+ ions with the different lignin sample solutions was monitored by absorbance measurement using a UV-vis spectrophotometer (Shimadzu, UV-1601 PC). The spectra of the surface plasmon resonance of AgNP in the samples were measured in 200-800 nm range with a resolution of 1 nm. The UV-vis spectra were recorded using a quartz cuvette with water as reference.

3.3.3 TRANSMISSION ELECTRON MICROSCOPY (TEM) ANALYSIS OF NANOPARTICLES

The nanoparticle size and morphology was analyzed by using transmission electron microscope (JEOL, JEM 1200EX-II) operating at 120 kV. TEM samples were prepared by placing a drop of the suspension of hybrid lignin/AgNP on carbon-coated copper grids and allowing water to evaporate at room temperature. The analysis of the selected area electron diffraction (SAED) patterns were analyzed using the CrysTBox software in order to identify the silver crystal planes and the corresponding d -spacings.

3.3.4 FOURIER-TRANSFORMED INFRARED (FT-IR) SPECTROSCOPY ANALYSIS

The changes in the surface chemical bonds and surface composition due to the possible participation of bioactive functional groups in capping and stabilization of nanoparticles after the bioreduction of silver were obtained using the Fourier Transform Infrared Spectrometer (Bruker, Vertex 70) with DRIFT (diffuse reflectance) accessory.

Reflectance technique was used with 64 scans, resolution of 4 cm⁻¹, without elimination of atmospheric compensation in the region between 4000 to 400 cm⁻¹. The dried samples were mixed with potassium bromide (KBr) in a ratio of 1:5 using an agate mortar and pestle Anthony et al. (2014).

3.3.5 DYNAMIC LIGHT SCATTERING (DLS) AND ZETA POTENTIAL OF NANOPARTICLES

The average size of AgNPs in aqueous medium was used to determine hydrodynamic diameter by DLS (Brookhaven, NanoDLS). For the analysis of Zeta potential, the resulting solutions of hybrid lignin/AgNPs were diluted with ultrapure water in a relation 2:3 to give a total volume of 10 mL. The analysis was carried out using a Zeta Potential analyzer (Stabino) with a 10 mL PTFE measurement cell and a 400 µm piston. The measurement of Zeta potential was done in a pH-titration mode using 0.05 M HCl and 0.05 M NaOH as titrants.

3.3.6 ANTIOXIDANT ACTIVITY

The antioxidant activity was measured using 2,2-diphenyl-2-picrylhydrazyl (DPPH) as free radical. The lignin solutions were tested at concentrations of 200, 100, 50 and 25 µg.mL⁻¹. In the case of the resulting solutions of hybrid lignin/AgNP, the concentrations tested were 100, 50, 25 and 12.5% diluted in water. The reactions took place by mixing 0.2 mL of tested compound with 0.8 mL of 0.1 mM DPPH (dissolved in methanol). The mixture was shaken vigorously and left to stand for 30 min in the dark before measuring the absorbance at 517 nm. Then the scavenging ability was calculated using the following equation (1):

$$\text{Equation (1)} \quad I (\%) = 100 \times \frac{(A_{control} - A_{sample})}{A_{control}}$$

Where I (%) is the inhibition percent, A_{control} is the absorbance of the control reaction (containing water as sample) and A_{sample} is the absorbance of the test compound Lateef et al. (2016) e Saravanakumar et al. (2015).

3.3.7 ANTIMICROBIAL ACTIVITY

3.3.7.1 DISK DIFFUSION TEST

Bacterial sensitivity to antibiotics is commonly tested using a disc diffusion test. The antimicrobial activity was done on pathogenic bacteria like *Escherichia coli* ATCC 35218. Mueller-Hinton agar (MHA) was used to cultivate Bacteria. Briefly, 100 μL (10^8 CFU mL^{-1}) of microbial culture was swabbed uniformly onto the individual plates using sterile cotton swabs. Then, sterile paper disc of 10 mm diameter containing 50 μL of hybrid lignin/AgNP solutions were placed on the MHA plates. The plates were incubated at 37°C for 24 h. After 24 h the diameter of the growth inhibition zones was measured Bindhu; Umadevi (2013).

3.3.7.2 MINIMUM INHIBITORY CONCENTRATION (MIC)

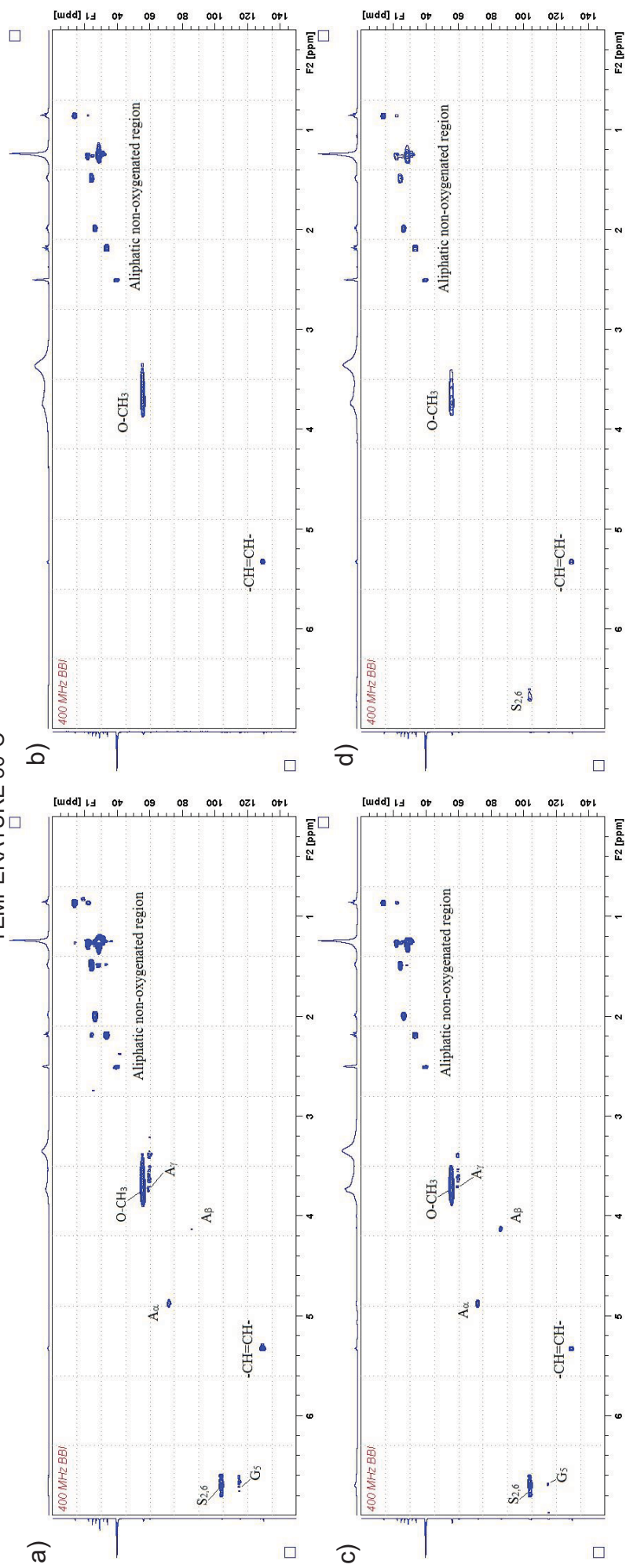
The antibacterial test was carried out via a growth inhibition assay. *Escherichia coli* ATCC 35218 was grown on Mueller-Hinton agar (MHA) at 37°C for overnight. The cultures were diluted in physiologic solution and adjusted to 0.5 McFarland scale. First, the cultures adjusted to 0.5 McFarland scale were diluted in Mueller-Hinton broth (MHB) to a concentration of 10^6 CFU mL^{-1} and 100 μL of antimicrobial agent were pipetted in the first row of a 96-well microplate. Then 50 μL of MHB were pipetted in each well from the second till the last row of the microplate. Serial two-dilutions of antimicrobial agent were made by pipetting 50 μL from the first row to the second one and repeating this from the 2nd to the 3rd and so on. The 8th row contained no antimicrobial agent. Finally, 50 μL of *E. coli* cells were inoculated in each well from the second until the 8th row. The final concentrations of antimicrobial agents (four lignins, AgNO_3 and HAL3-L AgNP) were 1000, 500, 250, 125, 62.5 and 31.25 $\mu\text{g}\cdot\text{mL}^{-1}$. The first row is considered as a negative growing control and the last row as a positive growing control. After 16 hours, 30 μL of resazurin ($10 \mu\text{g}\cdot\text{mL}^{-1}$) was added to every well and the microplate was incubated one hour more. The development of a pink color indicates no inhibitory activity at the tested concentration of antimicrobial agent.

4 RESULTS AND DISCUSSION

4.1 2D HSQC NMR CHARACTERIZATION

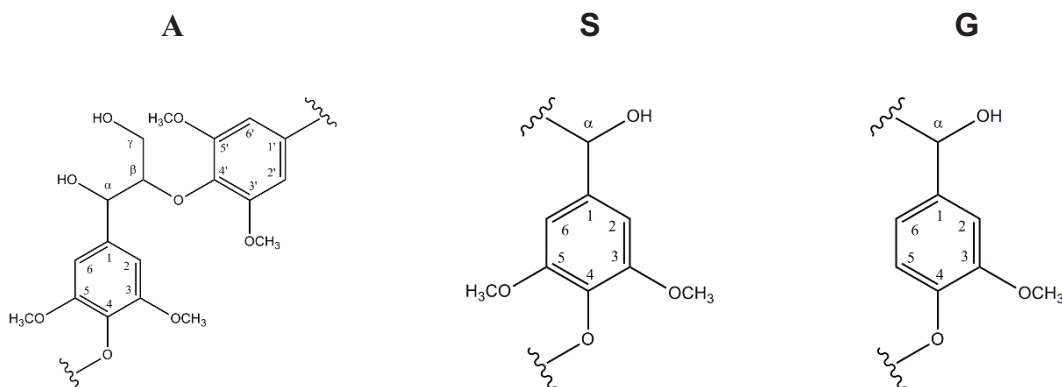
The 2D HSQC NMR spectra of the non-acetylated lignin samples are presented in figure 1, the main found structures are presented in figure 2 and the main cross-signal assignments are listed in table 2 by comparison with literature.

FIGURE 1 - 2D HSQC SPECTRA OF DIFFERENT LIGNIN SAMPLES: (a) HAL1-L; (b) HAL2-L; (c) HAL3-L; AND (d) HAL4-L. SOLVENT d6-DMSO. TEMPERATURE 30°C



SOURCE: The author (2017).

FIGURE 2 - MAIN STRUCTURES PRESENT IN OPEFB LIGNIN: (A) β -O-4' ARYL ETHER LINKAGES; (S) SYRINGYL UNITS AND (G) GUAIACYL UNITS



SOURCE: The author (2017).

TABLE 2 – ASSIGNMENTS OF ^{13}C - ^1H CORRELATION SIGNALS IN THE 2D HSQC NMR SPECTRA CORRESPONDING TO EACH NON-ACETYLATED LIGNIN SAMPLE

$\delta\text{C}/\delta\text{H}$				Assignment	Reference
HAL1-L	HAL2-L	HAL3-L	HAL4-L		
55.9/3.72	55.9/3.73	55.9/3.73	55.9/3.73	C-H in methoxyls (O-CH ₃)	Fernández-Costas et al. (2014)Toledano; García; et al. (2010)Singh; Dhepe (2016)
59.6/3.72		59.6/3.70		A γ : C γ -H γ in β -O-4' substructures	Rencoret et al. (2009)Fernández-Costas et al. (2014)Toledano; Serrano; et al. (2010)
72.2/4.87		72.2/4.87		A α : C α -H α in β -O-4' linked to a S units	Li et al. (2012)Rencoret et al. (2009) Fernández-Costas et al. (2014)
86.0/4.13		86.0/4.12		A β : C β -H β in β -O-4' linked to a S unit	Li et al. (2012)Rencoret et al. (2009)
104.3/6.70		104.2/6.69	104.3/6.69	S _{2,6} : C _{2,6} -H _{2,6} in S units	Fernández-Costas et al. (2014)Singh; Dhepe (2016)Schmetz et al. (2016)
115.5/6.66		115.5/6.68		G ₅ : C ₅ -H ₅ in G units	Singh; Dhepe (2016)
129.6/5.32	129.6/5.32	129.6/5.32	129.6/5.32	-CH=CH- structures	Singh; Dhepe (2016)

SOURCE: The author (2017).

In general, the HSQC NMR spectra for lignin samples can be separated into three regions whose signals correspond to aliphatic, side-chain and aromatic/olefin ^{13}C - ^1H correlations. The aliphatic (non-oxygenated) region ($\delta\text{C}/\delta\text{H}$ 10-50/0.5-2.5 ppm) showed signals corresponding to CH₃, CH₂ and H of the propyl chains and acetyl group present in lignin Coral Medina et al. (2016). These signals contribute with no structural or sufficient information to make distinction between the units present in lignin Rencoret et al. (2009 e Singh; Dhepe (2016). The side-chain (also known as aliphatic

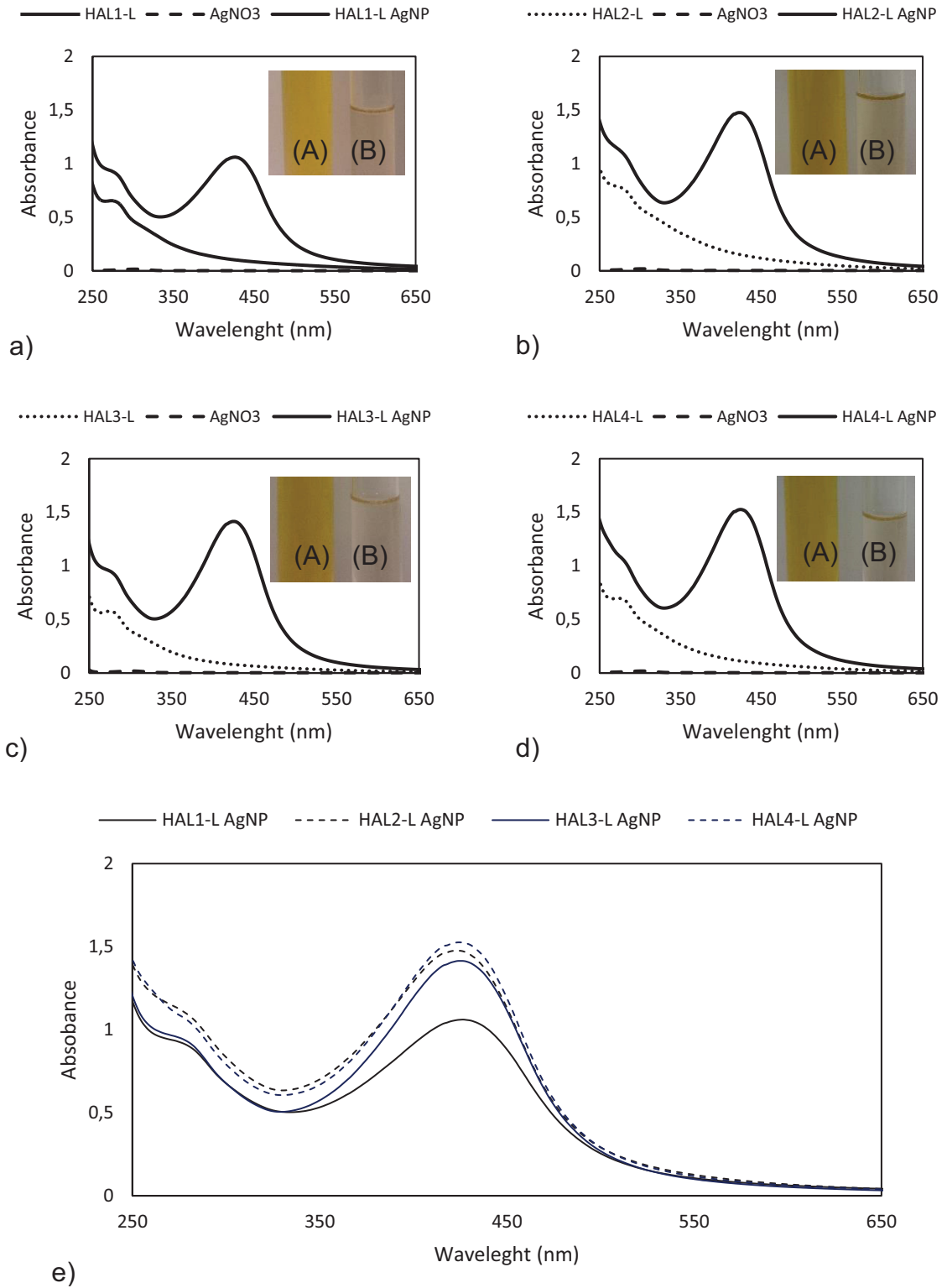
oxygenated) region ($\delta\text{C}/\delta\text{H}$ 50–95/2.5–6.0 ppm) gives useful information about the different inter-unit linkages present in OPEFB lignin. The most prominent signal presented at 55.9/3.73 ppm represents methoxyl groups Fernández-Costas et al. (2014). Other important signals corresponded to β -O-4' aryl ether linkages (substructure A) where $\text{C}\alpha\text{-H}\alpha$ and $\text{C}\beta\text{-H}\beta$ correlations were observed at $\delta\text{C}/\delta\text{H}$ 72.2/4.87 and 86.0/4.13 ppm for β -O-4' structures linked to S-lignin units, respectively. Also, the $\text{C}\gamma\text{-H}\gamma$ correlations in β -O-4' substructures were observed at $\delta\text{C}/\delta\text{H}$ 59.6/3.70 ppm Li et al. (2012 e Rencoret et al. (2009). It is important to mention that β -O-4' ether linkages were dramatically reduced during the biomass pre-treatment process (like in Kraft process) and their corresponding signals are not as predominant in the HSQC spectrum as they would be in the raw lignin Fernández-Costas et al. (2014). Phenylcoumaran structures are absent in all the spectra and the same occurs to their degradation products, ie. stilbene structures. Moreover, no resinol nor dibenzodioxocin substructures were found in any spectra Fernández-Costas et al. (2014). The main cross-signals found in the aromatic region ($\delta\text{C}/\delta\text{H}$ 95–160/5.5–8.5 ppm) of the HSQC spectrum corresponded principally to benzene rings of the lignin units, specifically from syringyl (S) lignin units. The C2,6-H2,6 correlation from the S-lignin unit exhibited a signal at $\delta\text{C}/\delta\text{H}$ 104.3/6.70 ppm Schmetz et al. (2016). Additionally, although a weak signal at $\delta\text{C}/\delta\text{H}$ 115.5/6.68 ppm could be attributed to the C5-H5 correlation in found in G units Singh; Dhepe (2016), a strong correlation corresponding to C2-H2 and C6-H6 were not found in any of the lignin samples. Although the signals of H-lignin units were not detected in the HSQC spectra, this information could be confirmed by Py-GC/MS analysis Rencoret et al. (2009). From the 2D HSQC NMR results, it was observed that lignins obtained under aggressive acid hydrolysis conditions (HAL2-L and HAL4-L) exhibited less cross-signals compared to those obtained under soft acid hydrolysis conditions (HAL1-L and HAL3-L) meaning a higher degree of degradation of the lignin complex structure.

4.2 VISUAL OBSERVATIONS AND UV-VISIBLE SPECTROSCOPY

In this study, the formation of silver nanoparticles (AgNPs) using lignin extracted from OPEFB at different acid hydrolysis conditions and subsequent alkaline extraction was investigated. The formation of silver nanoparticles using four different

lignins was confirmed by the change in color of the reaction solution from almost colorless to yellowish color. Refer to figure 3a-d, (tubes A and B).

FIGURE 3 - VISUAL OBSERVATION AND UV-VISIBLE SPECTRA OF REACTION MIXTURES (TUBE A) USING DIFFERENT LIGNINS (TUBE B): (a) HAL1-L, (b) HAL2-L, (c) HAL3-L AND (d) HAL4-L. (e) COMPARISON OF SURFACE PLASMON RESONANCE PEAKS OF AGNPS USING FOUR DIFFERENT LIGNINS.



SOURCE: The author (2017).

This observed phenomena is due to the excitation of surface plasmon vibrations in silver nanoparticles Mohan et al. (2014). The UV-visible spectra obtained using the four different lignins as reducing agent show the spectra of AgNPs very different from the spectra of the lignin and AgNO₃ used as initial reagents. A strong, broad peak located between 420 to 440 nm was observed in the resulting solutions of AgNPs and there is no clear change in the peak position using the four different lignins. The surface plasmon resonance (SPR) peaks for the four AgNPs exhibited a maximum absorbance at almost the same wavelength: 423-427. However, the lower absorbance value observed, the lower concentration of AgNP synthesized Chan; Mat Don (2013). Refer to table 3.

TABLE 3 – SURFACE PLASMON RESONANCE OF AgNPS USING FOUR DIFFERENT LIGNINS

Nanoparticle	Surface Plasmon resonance (nm)	Maximum absorbance
HAL1-L AgNP	427	1.1893
HAL2-L AgNP	424	1.9894
HAL3-L AgNP	425	1.5667
HAL4-L AgNP	425	1.9641

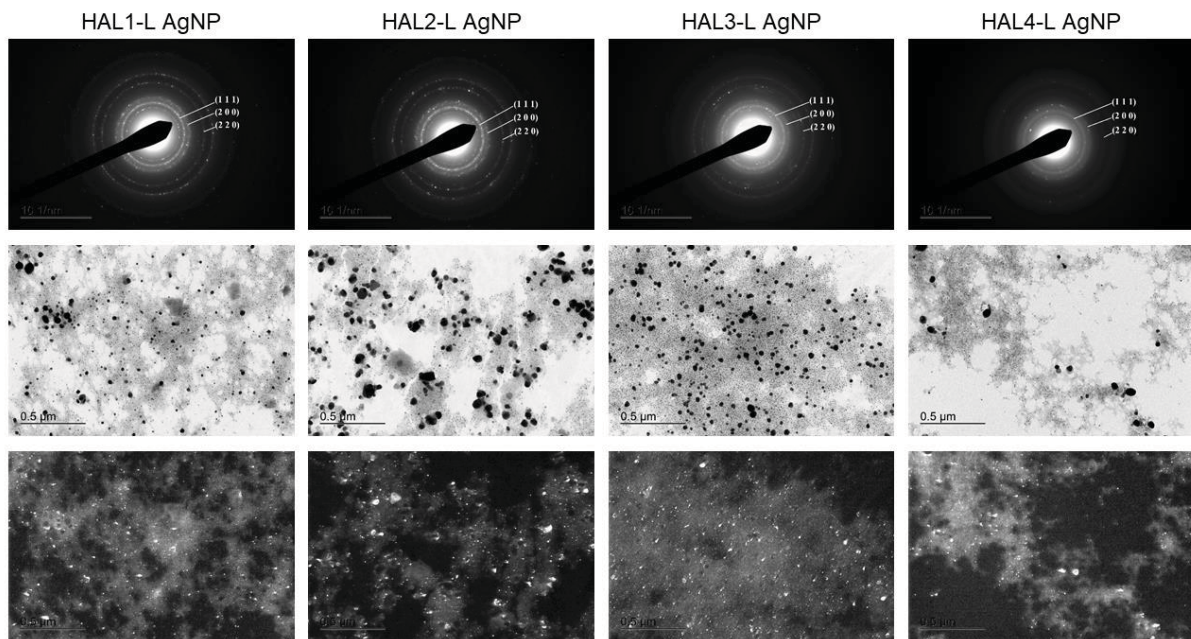
SOURCE: The author (2017).

Figure 3e revealed the effect of varying the lignin used on the nanoparticle synthesis. As the maximum absorbance of the surface plasmon peak corresponding to HAL1-L AgNP presented the lowest absorbance between the other nanoparticles, it could be said that lignin HAL1-L produced a much lower amount of AgNPs. Additionally, it was noticed that the lignins obtained under hard conditions (HAL2-L and HAL4-L) produced higher amount of AgNPs compared to the lignins obtained under soft conditions (HAL1-L and HAL3-L), possibly due to higher reducing power of the firsts ones. A slight difference in absorbance was also observed between lignins HAL1-L and HAL3-L, indicating that the use of H₂SO₄ in the acid hydrolysis decomposes lignin in a different way than HCl and increases the reducing power of lignin. As stated by Kelly et al. (2003), the surface plasmon resonance bands are influenced by size, shape, morphology, composition and dielectric environment of the prepared nanoparticles, other techniques like TEM, FT-IR, DLS and Zeta Potential were used to characterize the silver nanoparticles.

4.3 TRANSMISSION ELECTRON MICROSCOPY (TEM) ANALYSIS

In the bright field TEM images, the dark spots revealed that the synthesized AgNPs possess almost spherical morphology with very little agglomeration for all the four lignins used (Figure 4).

FIGURE 4 - BRIGHT FIELD TEM, DARK FIELD TEM AND SAED PATTERN SHOWING DIFFERENT CRYSTALLINE PATTERNS OF AgNPS SYNTHESIZED USING DIFFERENT LIGNINS



SOURCE: The author (2017).

The shining spots on the dark field TEM images shows that not all the particles on the bright field TEM images possess metallic silver in its interior but confirms that most of them are real AgNPs. The selected area electron diffraction (SAED) pattern revealed the polycrystalline nature of the nanoparticles and indicated they were crystals of face-centered cubic (fcc) silver. The diffraction rings, from inner to outer, corresponded to (111), (200) and (220) planes of fcc structure of silver. The lattice spacing (d) calculated for each plane of the AgNPs synthesized with different lignins are presented in table 4 Ajitha et al. (2014 e Mohan et al. (2014).

TABLE 4 – LATTICE SPACING (d) OF AgNPS SYNTHESIZED WITH DIFFERENT LIGNINS

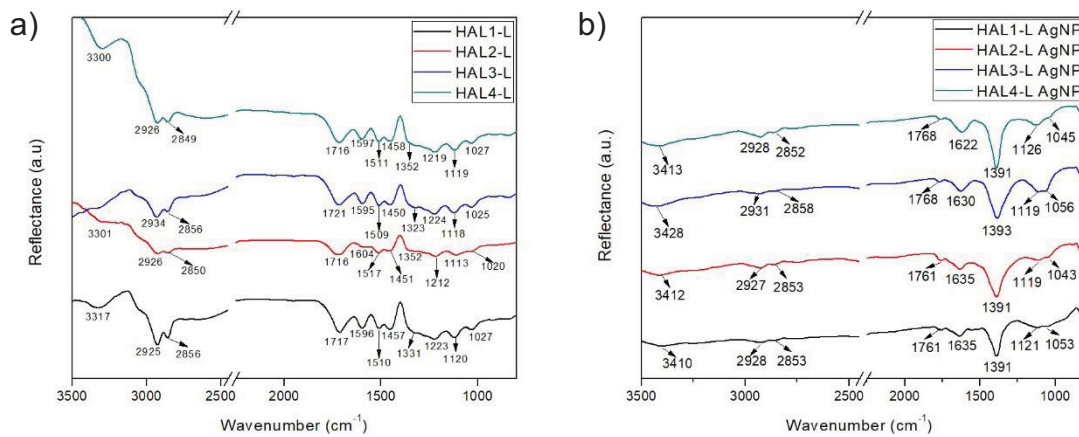
Plane (Bragg reflections)	Theoretical d -spacing	Calculated d -spacing			
		HAL1-L AgNP	HAL2-L AgNP	HAL3-L AgNP	HAL4-L AgNP
2 2 0	0.145	0.137	0.138	0.137	0.137
2 0 0	0.204	0.195	0.197	0.198	0.195
1 1 1	0.236	0.225	0.227	0.227	0.227

SOURCE: The author (2017).

4.4 FOURIER-TRANSFORMED INFRARED (FT-IR) SPECTROSCOPY ANALYSIS

IR spectrum helps in identifying specific functional groups present in the synthesized AgNPs which play the roles of capping agent and reducing agent. As shown in figure 5, there are various reflectance signals located at specific wavenumbers (cm^{-1}) for the four lignins used and the corresponding synthesized AgNPs.

FIGURE 5 - FT-IR SPECTRA OF (a) LIGNINS AND (b) SILVER NANOPARTICLES SYNTHESIZED WITH DIFFERENT LIGNINS



SOURCE: The author (2017).

The characteristic absorption frequencies of lignins and AgNPs synthesized are reported in table 5.

TABLE 5 – FT-IR STRETCHING FREQUENCIES FOUND ON LIGNINS AND CORRESPONDING AgNPS

Lignin stretching frequencies (cm ⁻¹)	AgNPs stretching frequencies (cm ⁻¹)	Type of bond	Reference
3317 – 3301	3428 – 3410	Aromatic and aliphatic O-H stretching	Boeriu et al. (2004)
2934 – 2925	2931 – 2927	C-H aliphatic stretching in (-OCH ₃), (-CH ₃) and (=CH ₂ /-CH ₂ -) groups	Singh; Dhepe (2016)
2856 – 2849	2858 – 2852	C-H aliphatic stretching in (-OCH ₃), (-CH ₃) and (=CH ₂ /-CH ₂ -) groups	Singh; Dhepe (2016)
1721 – 1716	1768 – 1761	C=O (in carbonyl compounds)	Hage et al. (2009)
1604 – 1595	1635 – 1622	C=O (in carbonyl compounds)	Gosselink et al. (2004)
1517 – 1509		C-H stretching in aromatic rings	Gosselink et al. (2004)
1458 – 1450		C-H asymmetric deformations in –CH ₃ and –CH ₂ –	Singh; Dhepe (2016)
1352 – 1323	1393 – 1391	Signals associated to syringyl and guaiacyl groups	García et al. (2009)
1224 – 1212		Signals associated to syringyl and guaiacyl groups	García et al. (2009)
1120 – 1113	1126 – 1119	Signals associated to syringyl and guaiacyl groups	García et al. (2009)
1027 – 1020	1056 – 1043	Various vibrations like C-O, C-H and C=O	Gosselink et al. (2004)

SOURCE: The author (2017).

In the present study, the strong and broad peak at 3300-3400 cm⁻¹ indicates the presence of hydroxyl groups (O-H stretching) in aliphatic and aromatic structures Boeriu et al. (2004). The peaks located between 3000 and 2800 cm⁻¹ can be attributed to C-H aliphatic stretching in methoxyl (-OCH₃), in methyl (-CH₃) and methylene (=CH₂/-CH₂-) groups of the propyl side chain present in lignins Singh; Dhepe (2016). The medium peaks from 1768 to 1595 cm⁻¹ refer to the carbonyl (C=O) stretching vibrations Gosselink et al. (2004 e Hage et al. (2009). The peaks at 1517-1509 cm⁻¹ found on the lignins are attributed to C-H stretching in aromatic rings Gosselink et al. (2004) and the signals at 1458-1450 cm⁻¹ correspond to asymmetric C-H deformations in –CH₃ and –CH₂– Singh; Dhepe (2016). The signals (1390-1330, 1224-1219 and 1126-1113 cm⁻¹) associated to syringyl and guaiacyl groups were also identified in the all four lignins and only some of those peaks were also found in AgNPs spectra García et al. (2009). The peaks at 1056-1020 cm⁻¹ can be attributed to various vibrations like C-O, C-H and C=O Gosselink et al. (2004). It was not possible to find notable differences between the four lignins extracted from OPEFB. In the case of silver nanoparticles, all of them present the same functional groups between them. It was noticed that some signals present on the lignin samples did not appeared on the

AgNPs spectra, possibly due to the electrostatic cross-linking that occurred between lignin and AgNPs Aadil et al. (2016).

4.5 PARTICLE SIZE DISTRIBUTION

The hydrodynamic diameter of the four lignin-mediated AgNPs were measured by dynamic light scattering (DLS). The average size of AgNPs in coloidal solutions are detailed in table 6.

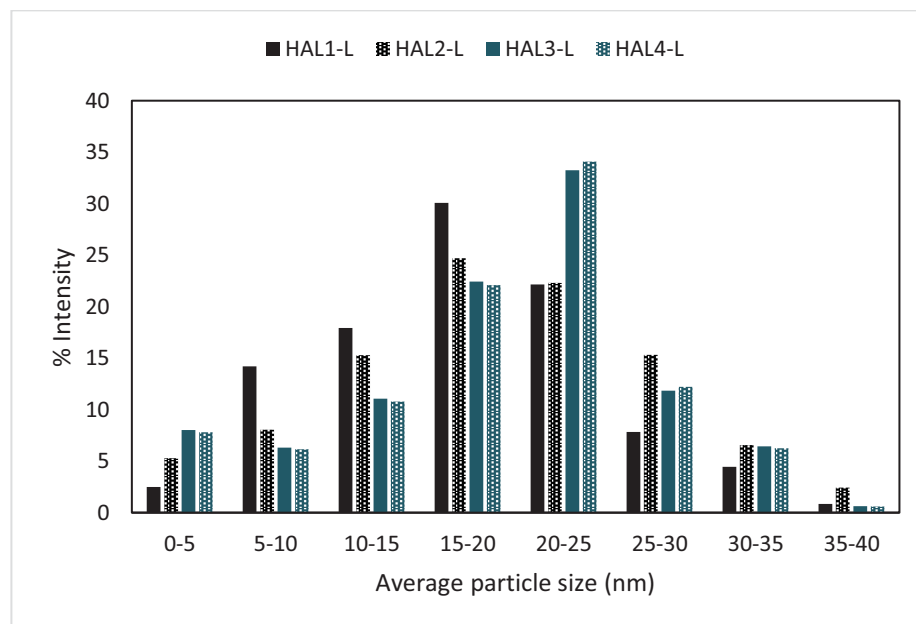
TABLE 6 – AVERAGE PARTICLE SIZE OF AgNPS SYNTHESIZED WITH DIFFERENT LIGNINS

Silver nanoparticle	Average particle size (nm)
HAL1-L AgNP	17.63
HAL2-L AgNP	19.24
HAL3-L AgNP	19.09
HAL4-L AgNP	19.19

SOURCE: The author (2017).

Although the four AgNPs present almost the same value of average particle size of 18.79 nm, figure 6 shows differences in the AgNPs size distribution. Well-dispersed AgNPs were found and the figure reveals that the particles ranged in size from 1 to 40 nm.

FIGURE 6 - AVERAGE PARTICLE SIZE DISTRIBUTION OF AGNPS USING DIFFERENT LIGNINS AS REDUCING AGENT: HAL1-L, HAL2-L, HAL3-L AND HAL4-L.



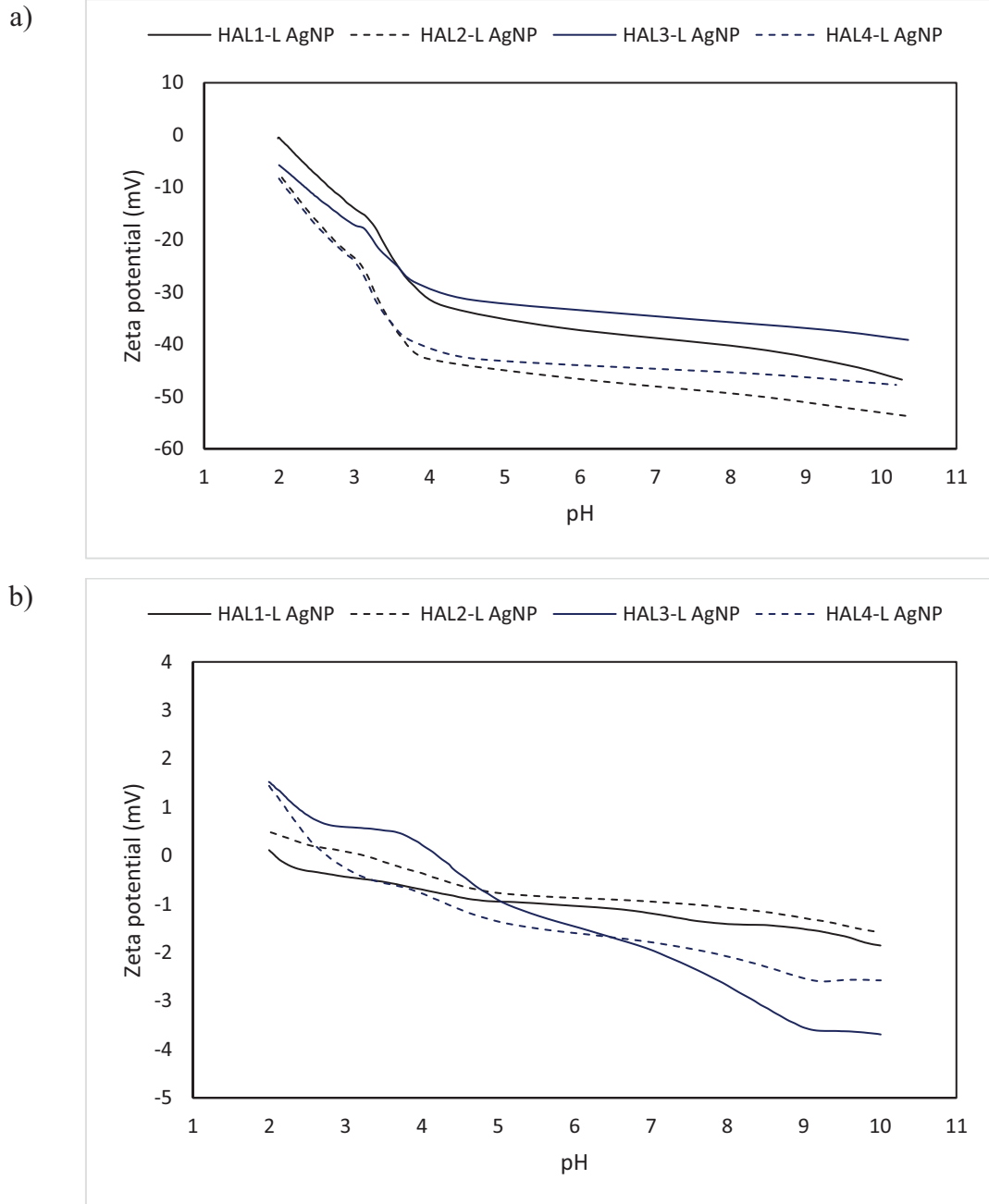
SOURCE: The author (2017).

Figure 6 also shows that HAL1-L AgNP possess most of its particles in the range between 15-20 nm while HAL3-L and HAL4-L AgNPs present similar size distribution pattern with most of its particles size between 20-25 nm. In the case of HAL2-L AgNP, most of its particles are distributed between 15-25 nm. Aadil et al. (2016) using lignin extracted from Acacia wood powder produced AgNPs with average diameter of 100 nm. Furthermore, Milczarek et al. (2013) reported a mean size of 46 nm for the AgNPs synthesized using a commercial sodium softwood lignosulphonate obtained from Borregaard LignoTech. Comparing other green methods for the AgNPs synthesis, Sankar et al. (2013) found that silver nanoparticles synthesized from *Origanum vulgare* leaf extract showed sizes ranging from 63 to 85 nm. While, Sriranjani et al. (2016) reported the use *Clerodendrum phlomidis* leaf extract as reducing agent producing AgNPs with sizes ranging between 10 to 15 nm. Also, Nanda; Saravanan (2009) showed that the biosynthesized AgNPs produced by *Staphylococcus aureus* agglomerated and formed different nanostructures with particle sizes ranging from 160 to 180 nm.

4.6 ZETA POTENTIAL

The stability of a silver nanoparticle colloidal solution is characterized by the zeta potential value. Generally, a nanoparticle suspension that exhibits an absolute zeta potential less than 20 mV is considered unstable and will result in precipitation of particles from solution Sun et al. (2014). By contrary, high zeta potential absolute value designates high electrical charge on the surface of the nanoparticles, causing strong repulsive force among the particles for withholding agglomeration Guo et al. (2015). In figure 7a, the Zeta potential profiles exhibited by the four lignin-mediated AgNPs diluted in ultrapure water were almost the same. The differences observed between the four profiles could be principally attributed to a little higher concentration of unreacted silver ions present in samples like HAL1-L AgNP and HAL3-L AgNP.

FIGURA 7 - ZETA POTENTIAL AS A FUNCTION OF pH FOR AgNPS SYNTHESIZED USING DIFFERENT LIGNINS: HAL1-L, HAL2-L, HAL3-L, HAL4-L. A) AGNPS DISSOLVED IN ULTRAPURE WATER AND B) IN MUELLER-HINTON BROTH



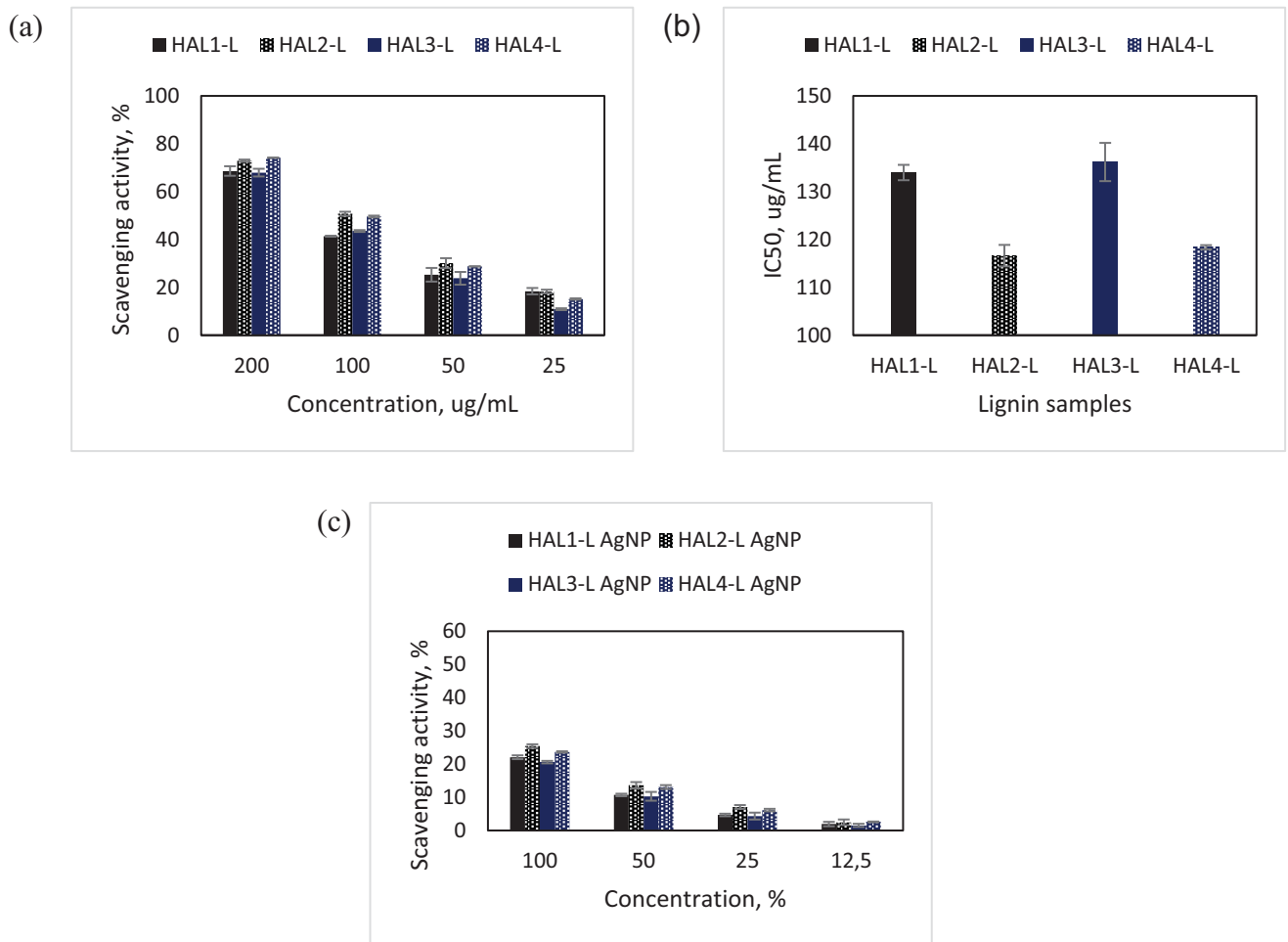
The four lignin-mediated AgNPs possessed high stability in aqueous solution showing absolute Zeta potential values higher than 20 mV at pH higher than 4. Aadil et al. (2016) reported that the AgNPs produced with lignin extracted from Acacia wood powder presented a Zeta potential value of -8.64 mV. Additionally, Prathna et al. (2011) showed that AgNPs synthesized using Citrus limon (lemon) aqueous extract presented a Zeta potential of -29 mV at a pH of 3.97. Also, Sankar et al. (2013) reported a Zeta potential of -26.0 mV for a plant-mediated AgNPs using *Origanum vulgare*. It is important to mention that as the AgNPs were intended to be used in much complex solutions like culture media, the Zeta potential profiles were also examined diluting the AgNPs in Mueller-Hinton broth instead of ultrapure water. Figure 7b showed that the four lignin-mediated AgNPs presented the same profile with Zeta potential values very close to 0 mV in a pH range from 2 to 10. This result implies that the AgNPs in solutions with much higher ions content could result to the instability of the colloidal suspension and finally agglomeration of the particles. However, the instability or agglomeration of AgNPs does not necessarily imply that silver ions would not be released but in an agglomerate state, the nanoparticles would exhibit a different biological behavior depending on the size, shape and surface chemistry Liu et al. (2010). Additionally, another important fact is that the AgNPs presented a negative Zeta potential value at pH higher than 5 and as their antimicrobial action stems from the localized emission of Ag⁺ ions at the cell membranes of microbes, their surface charge is probably the main facilitator of this biological activity Richter et al. (2015). Due to the negatively charged bacterial cell membranes, a charge inversion of the surface of AgNPs from negative to positive would be necessary and accomplished by functionalization of the surface of the nanoparticles Ravindran et al. (2013).

4.7 ANTIOXIDANT ACTIVITY (DPPH)

Figure 8 exhibits the antioxidant activities of the four lignins extracted from OPEFB and the resulting solutions of AgNPs diluted in water. From figure 8a, it can be seen that the lignins extracted under aggressive acid hydrolysis conditions (HAL2-L and HAL4-L) using either HCl or H₂SO₄ exhibits higher scavenging activity that those lignins extracted under soft conditions. This could be attributed to a higher amount of more reducing functional groups on the chemical structure of lignins HAL2-L and HAL4-L. As the 2D HSCQ NMR results indicated a higher degradation of lignins HAL2-L and HAL4-L compared to HAL1-L and HAL3-L, it also mean a higher presence of

reducing functional groups in their structure. Additionally, the concentration of lignin that inhibited 50% of the free-radical (IC₅₀) was calculated.

FIGURA 8 - ANTIOXIDANT ACTIVITY (DPPH): (A) SCAVENGING ACTIVITY OF LIGNINS AT DIFFERENT CONCENTRATIONS (200, 100, 50 AND 25 $\mu\text{g}\cdot\text{mL}^{-1}$); (B) INHIBITORY CONCENTRATION OF 50% OF FREE-RADICAL BY DIFFERENT LIGNINS; (C) SCAVENGING ACTIVITY OF RESULTING SOLUTIONS FROM THE SYNTHESIS OF AgNPS DIFFERENT CONCENTRATIONS (100, 50, 25 AND 12.5%).



SOURCE: The author (2017).

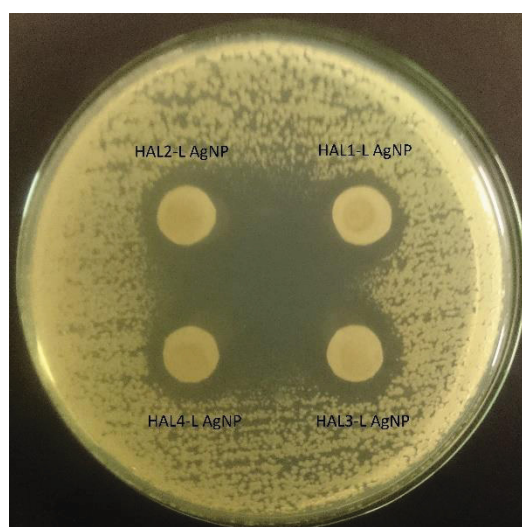
Figure 8b shows the IC₅₀ corresponding to each lignin ample: 134, 117, 136 and 118 $\mu\text{g}\cdot\text{mL}^{-1}$, corresponding to HAL1-L, HAL2-L, HAL3-L and HAL4-L, respectively. As stated lines above, lignins HAL2-L and HAL4-L exhibit higher reducing power than HAL1-L and HAL3-L. Additionally, the antioxidant activity of the resulting solutions of the hybrid lignin/AgNPs diluted with water was calculated. From figure 8c, it can be observed that the hybrid lignin/AgNP solution exhibits the same

inhibitory activity as the solutions of lignin at the same concentrations. As the antioxidant activity of silver nitrate was also estimated and exhibited no inhibitory capacity (data not presented), it could be said that lignins conferees antioxidant capacities to the corresponding AgNPs synthesized.

4.8 ANTIMICROBIAL ACTIVITY

The antibacterial activity of lignins, AgNO₃ and AgNPs against *E. coli* was investigated. The disk-diffusion method was used to evaluate differences between the inhibition zones developed by the four different resulting solutions of hybrid lignin/AgNPs (Figure 9). Refer to table 7 for inhibitions zones developed for each hybrid lignin/AgNP.

FIGURA 9 - ANTIMICROBIAL ACTIVITY – DISK DIFFUSION METHOD COMPARING THE RESULTING SOLUTIONS OF SILVER NANOPARTICLES SYNTHESIZED WITH DIFFERENT LIGNINS: HAL1-L, HAL2-L, HAL3-L AND HAL4-L



SOURCE: The author (2017).

TABLE 7 – INHIBITION ZONES DEVELOPED BY DIFFERENT AgNPS AGAINST *Escherichia coli* ATCC 35218

Silver nanoparticle	Inhibition zone (mm)
HAL1-L AgNP	18.7 ± 0.60
HAL2-L AgNP	19.3 ± 0.58
HAL3-L AgNP	18.7 ± 0.58
HAL4-L AgNP	18.7 ± 0.58

SOURCE: The author (2017).

As no significant difference were observed between the four tested AgNPs, HAL3-L AgNP was chosen to be evaluated by minimum inhibitory concentration (MIC) because the lignin used came from a soft hydrolysis process. HAL3-L AgNP resulting solution was dialyzed using a 1 kDa cut-off membrane and ultrapure water for 48 hours.

For the MIC experiment, the four lignins, silver nitrate and HAL3-L AgNP were tested as antimicrobial agent in a 96-well microplate (Figure 10). All substances were tested at the same concentrations. For the four lignins, it was not possible to establish a MIC as the microorganism was able to grow even at the maximum concentration tested (1000 $\mu\text{g}\cdot\text{mL}^{-1}$). This result does not mean that lignin did not present any inhibitory effect on the growth of the microorganism but it could possibly reduce the number of viable cells able to grow. By contrary, the AgNO_3 exhibited a visible inhibitory effect even at the lowest concentrations tested (31.25 $\mu\text{g}\cdot\text{mL}^{-1}$). In the case of the silver nanoparticle solution (HAL3-L AgNP), it was possible to establish that a concentration of 62.5 $\mu\text{g}\cdot\text{mL}^{-1}$ inhibited the visible growth of the microorganism tested (MIC). Other researches like Wani et al. (2013) reported that the AgNPs synthesized by microemulsion method exhibited a higher MIC of 100 $\mu\text{g}\cdot\text{mL}^{-1}$. On the other hand, Balakumaran et al. (2016) reported that the "green" AgNPs synthesized using fungal extracts exhibited a MIC of 3.125 $\mu\text{g}\cdot\text{mL}^{-1}$. This lower MIC result was attributed to the binding of proteins with AgNPs which could result in a much higher biocompatibility and increase in antimicrobial activity. In general, the mechanism of cellular toxicity exhibited by metal nanoparticles is thought the release of reactive oxygen species (ROS) Nel et al. (2009). The exact antimicrobial mechanism of silver nanoparticles are still unclear but it is believed that the antimicrobial effect depends strongly of the superficial contact between silver and microorganisms Chan; Mat Don (2013). On the other hand, silver nanoparticles have been found to penetrate the bacterial cell membranes causing membrane cell damage and death of the organisms Ravindran et al. (2013) e Sun et al. (2014). A better understanding of the bactericidal action of the AgNPs would require an adequate examination of the membrane-bound and intracellular nanoparticles. Additionally, it is important to mention that the control over the size, shape and the surrounding environment of nanoparticles is a vital phenomenon that will determine most of their fundamental properties, including the antimicrobial effect Jeyaraj et al. (2013). As mentioned lines above, the Zeta potential value exhibited by AgNPs at pH values higher than 5 were negative and very close to 0 mV when dissolved in MHB. From this, it can be assumed that there is a sort of

repulsion between the AgNPs and the negatively charged bacterial cell membranes leading to a no localized release of silver ions. Finally, the charge inversion of the surface of the AgNPs could result in a much higher antimicrobial activity.

5 CONCLUSIONS

To conclude, we have taken advantage of an agricultural waste material finding an application that could increase the profitability of biomass production. A higher degradation on the chemical structure was found on those lignin samples that were obtained after submitting the OPEFB under hard hydrolysis conditions, observing less cross-signals on the 2D HSCQ NMR analysis. The synthesis of silver nanoparticles (AgNPs) was successfully achieved using lignin extracted from OPEFB as reducing and capping agent. It has been reported that the four lignins were able to produce mostly spherical shape nanoparticles with particle size distribution in the range of 1-40 nm, with functional groups from lignins capped on the surface. In a medium containing low ions concentration, all four AgNPs exhibit almost the same Zeta potential profile and a good stability at pH values higher than 4. On the other hand, in a medium with much higher ion concentration as the AgNPs exhibited a Zeta potential near to 0 mV. About the antioxidant activity exhibited by AgNPs, it seems that lignins confere their antioxidant capacity to the corresponding AgNPs as the silver nitrate solutions did not exhibit such behavior alone. Comparing the antimicrobial activity the four synthesized AgNPs, it was not observed a significant difference between the inhibitions zones developed against *E. coli* ATCC 35218. Therefore, HAL3-L AgNP was dialyzed and its MIC was found to be 62.5 $\mu\text{g}\cdot\text{mL}^{-1}$ against the same microorganism used on the disk-diffusion method.

REFERENCES

- AADIL, K. R.; BARAPATRE, A.; MEENA, A. S.; JHA, H. Hydrogen peroxide sensing and cytotoxicity activity of Acacia lignin stabilized silver nanoparticles. **International Journal of Biological Macromolecules**, v. 82, p. 39–47, 2016. Elsevier B.V. Disponível em: <<http://dx.doi.org/10.1016/j.ijbiomac.2015.09.072>>. .
- AADIL, K. R.; BARAPATRE, A.; SAHU, S.; JHA, H.; TIWARY, B. N. Free radical scavenging activity and reducing power of Acacia nilotica wood lignin. **International Journal of Biological Macromolecules**, v. 67, p. 220–227, 2014. Elsevier B.V. Disponível em: <<http://dx.doi.org/10.1016/j.ijbiomac.2014.03.040>>. .
- AJITHA, B.; ASHOK KUMAR REDDY, Y.; SREEDHARA REDDY, P. Biosynthesis of silver nanoparticles using Plectranthus amboinicus leaf extract and its antimicrobial activity. **Spectrochimica Acta - Part A: Molecular and Biomolecular Spectroscopy**, v. 128, p. 257–262, 2014. Elsevier B.V. Disponível em: <<http://dx.doi.org/10.1016/j.saa.2014.02.105>>. .
- ALI, K.; DWIVEDI, S.; AZAM, A.; et al. Aloe vera extract functionalized zinc oxide nanoparticles as nanoantibiotics against multi-drug resistant clinical bacterial isolates. **Journal of Colloid and Interface Science**, v. 472, p. 145–156, 2016. Elsevier Inc. Disponível em: <<http://dx.doi.org/10.1016/j.jcis.2016.03.021>>. .
- AMOOAGHAIE, R.; SAERI, M. R.; AZIZI, M. Synthesis, characterization and biocompatibility of silver nanoparticles synthesized from Nigella sativa leaf extract in comparison with chemical silver nanoparticles. **Ecotoxicology and Environmental Safety**, v. 120, p. 400–408, 2015. Elsevier. Disponível em: <<http://dx.doi.org/10.1016/j.ecoenv.2015.06.025>>. .
- ANTHONY, K. J. P.; MURUGAN, M.; JEYARAJ, M.; RATHINAM, N. K.; SANGILYANDI, G. Synthesis of silver nanoparticles using pine mushroom extract: A potential antimicrobial agent against E. coli and B. subtilis. **Journal of Industrial and Engineering Chemistry**, v. 20, n. 4, p. 2325–2331, 2014. The Korean Society of Industrial and Engineering Chemistry. Disponível em: <<http://dx.doi.org/10.1016/j.jiec.2013.10.008>>. .
- AZEREDO, H. M. C.; ROSA, M. F.; MATTOSO, L. H. C. Nanocellulose in bio-based food packaging applications. **Industrial Crops and Products**, p. 1–8, 2015. Elsevier B.V. Disponível em: <<http://dx.doi.org/10.1016/j.indcrop.2016.03.013>>. .
- BALAKUMARAN, M. D.; RAMACHANDRAN, R.; BALASHANMUGAM, P.; MUKESHKUMAR, D. J.; KALAICHELVAN, P. T. Mycosynthesis of silver and gold nanoparticles: Optimization, characterization and antimicrobial activity against human pathogens. **Microbiological Research**, v. 182, p. 8–20, 2016. Elsevier GmbH. Disponível em: <<http://dx.doi.org/10.1016/j.micres.2015.09.009>>. .
- BINDHU, M. R.; UMADEVI, M. Synthesis of monodispersed silver nanoparticles using Hibiscus cannabinus leaf extract and its antimicrobial activity. **Spectrochimica Acta - Part A: Molecular and Biomolecular Spectroscopy**, v. 101, p. 184–190, 2013. Elsevier B.V. Disponível em: <<http://dx.doi.org/10.1016/j.saa.2012.09.031>>. .
- BINDHU, M. R.; UMADEVI, M. Antibacterial and catalytic activities of green synthesized silver nanoparticles. **Spectrochimica Acta - Part A: Molecular and**

Biomolecular Spectroscopy, v. 135, p. 373–378, 2015. Elsevier B.V. Disponível em: <<http://dx.doi.org/10.1016/j.saa.2014.07.045>>. .

BOERIU, C. G.; BRAVO, D.; GOSSELINK, R. J. A.; VAN DAM, J. E. G. Characterisation of structure-dependent functional properties of lignin with infrared spectroscopy. **Industrial Crops and Products**, v. 20, n. 2, p. 205–218, 2004.

BOERIU, C. G.; FITIGAU, F. I.; GOSSELINK, R. J. A.; et al. Fractionation of five technical lignins by selective extraction in green solvents and characterisation of isolated fractions. **Industrial Crops and Products**, v. 62, p. 481–490, 2014.

BOERJAN, W.; RALPH, J.; BAUCHER, M. Lignin Biosynthesis. **Annual Review of Plant Biology**, v. 54, n. 1, p. 519–546, 2003. Disponível em: <<http://www.annualreviews.org/doi/10.1146/annurev.arplant.54.031902.134938>>. .

CAPANEMA, E. A.; BALAKSHIN, M. Y.; KADLA, J. F. Quantitative Characterization of a Hardwood Milled Wood Lignin by Nuclear Magnetic Resonance Spectroscopy. **Journal of Agricultural and Food Chemistry**, v. 53, p. 9639–9649, 2005.

CASTRO-MAYORGA, J. L.; MARTÍNEZ-ABAD, A.; FABRA, M. J.; et al. Stabilization of antimicrobial silver nanoparticles by a polyhydroxyalkanoate obtained from mixed bacterial culture. **International Journal of Biological Macromolecules**, v. 71, p. 103–110, 2014. Elsevier B.V. Disponível em: <<http://dx.doi.org/10.1016/j.ijbiomac.2014.06.059>>. .

CHAN, Y. S.; MAT DON, M. Biosynthesis and structural characterization of Ag nanoparticles from white rot fungi. **Materials Science and Engineering C**, v. 33, n. 1, p. 282–288, 2013. Elsevier B.V. Disponível em: <<http://dx.doi.org/10.1016/j.msec.2012.08.041>>. .

CORAL MEDINA, D. J.; LORENCI WOICIECHOWSKI, A.; ZANDONA FILHO, A.; et al. Biological activities and thermal behavior of lignin from oil palm empty fruit bunches as potential source of chemicals of added value. **Industrial Crops & Products**, v. 94, p. 630–637, 2016. Elsevier B.V. Disponível em: <<http://dx.doi.org/10.1016/j.indcrop.2016.09.046>>. .

CORAL MEDINA, J. D.; WOICIECHOWSKI, A.; ZANDONA FILHO, A.; et al. Lignin preparation from oil palm empty fruit bunches by sequential acid/alkaline treatment - A biorefinery approach. **Bioresource Technology**, v. 194, p. 172–178, 2015. Elsevier Ltd. Disponível em: <<http://dx.doi.org/10.1016/j.biortech.2015.07.018>>. .

EL-RAFIE, H. M.; EL-RAFIE, M. H.; ZAHRAN, M. K. Green synthesis of silver nanoparticles using polysaccharides extracted from marine macro algae. **Carbohydrate Polymers**, v. 96, n. 2, p. 403–410, 2013. Elsevier Ltd. Disponível em: <<http://dx.doi.org/10.1016/j.carbpol.2013.03.071>>. .

FERNÁNDEZ-COSTAS, C.; GOUVEIA, S.; SANROMAMÁN, M. A.; MOLDES, D. Structural characterization of Kraft lignins from different spent cooking liquors by 1D and 2D Nuclear Magnetic Resonance spectroscopy. **Biomass and Bioenergy**, v. 63, p. 156–166, 2014.

GARCÍA, A.; TOLEDANO, A.; SERRANO, L.; et al. Characterization of lignins obtained by selective precipitation. **Separation and Purification Technology**, v. 68, n. 2, p. 193–198, 2009.

GHAEDI, M.; YOUSEFINEJAD, M.; SAFARPOOR, M.; KHAFRI, H. Z.; PURKAIT, M. K. Rosmarinus officinalis leaf extract mediated green synthesis of silver nanoparticles and investigation of its antimicrobial properties. **Journal of Industrial and Engineering Chemistry**, v. 31, p. 167–172, 2015. The Korean Society of Industrial and Engineering Chemistry. Disponível em: <<http://dx.doi.org/10.1016/j.jiec.2015.06.020>>. .

GHOREISHI, S. M.; BEHPOUR, M.; KHAYATKASHANI, M. Green synthesis of silver and gold nanoparticles using Rosa damascena and its primary application in electrochemistry. **Physica E: Low-Dimensional Systems and Nanostructures**, v. 44, n. 1, p. 97–104, 2011. Elsevier. Disponível em: <<http://dx.doi.org/10.1016/j.physe.2011.07.008>>. .

GOSSELINK, R. J. A.; ABÄCHERLI, A.; SEMKE, H.; et al. Analytical protocols for characterisation of sulphur-free lignin. **Industrial Crops and Products**, v. 19, n. 3, p. 271–281, 2004.

GUO, D.; DOU, D.; GE, L.; et al. A caffeic acid mediated facile synthesis of silver nanoparticles with powerful anti-cancer activity. **Colloids and Surfaces B: Biointerfaces**, v. 134, p. 229–234, 2015. Elsevier B.V. Disponível em: <<http://dx.doi.org/10.1016/j.colsurfb.2015.06.070>>. .

GURUNATHAN, S. Biologically synthesized silver nanoparticles enhances antibiotic activity against Gram-negative bacteria. **Journal of Industrial and Engineering Chemistry**, v. 29, p. 217–226, 2015. The Korean Society of Industrial and Engineering Chemistry. Disponível em: <<http://dx.doi.org/10.1016/j.jiec.2015.04.005>>. .

HAGE, R. EL; BROSSE, N.; CHRUSCIEL, L.; et al. Characterization of milled wood lignin and ethanol organosolv lignin from miscanthus. **Polymer Degradation and Stability**, v. 94, n. 10, p. 1632–1638, 2009. Elsevier Ltd. Disponível em: <<http://dx.doi.org/10.1016/j.polyimdegradstab.2009.07.007>>. .

HOSSEINI, E. S.; WAHID, M. A. Utilization of palm solid residue as a source of renewable and sustainable energy in Malaysia. **Renewable and Sustainable Energy Reviews**, v. 40, p. 621–632, 2014. Elsevier. Disponível em: <<http://dx.doi.org/10.1016/j.rser.2014.07.214>>. .

HU, S.; HSIEH, Y. LO. Silver nanoparticle synthesis using lignin as reducing and capping agents: A kinetic and mechanistic study. **International Journal of Biological Macromolecules**, v. 82, p. 856–862, 2016. Elsevier B.V. Disponível em: <<http://dx.doi.org/10.1016/j.ijbiomac.2015.09.066>>. .

JEYARAJ, M.; VARADAN, S.; ANTHONY, K. J. P.; et al. Antimicrobial and anticoagulation activity of silver nanoparticles synthesized from the culture supernatant of Pseudomonas aeruginosa. **Journal of Industrial and Engineering Chemistry**, v. 19, n. 4, p. 1299–1303, 2013. The Korean Society of Industrial and Engineering Chemistry. Disponível em: <<http://dx.doi.org/10.1016/j.jiec.2012.12.031>>. .

KELLY, K. L.; CORONADO, E.; ZHAO, L. L.; SCHATZ, G. C. The Optical Properties of Metal Nanoparticles: The Influence of Size, Shape, and Dielectric Environment. **Journal of Physical Chemistry B**, v. 107, n. 3, p. 668–677, 2003.

KHALILZADEH, M. A.; BORZOO, M. Green synthesis of silver nanoparticles using onion extract and their application for the preparation of a modified electrode

for determination of ascorbic acid. **Journal of Food and Drug Analysis**, v. 24, n. 4, p. 796–803, 2016. Elsevier Ltd. Disponível em: <<http://dx.doi.org/10.1016/j.jfda.2016.05.004>>. .

KURIHARA, K.; ROCKSTUHL, C.; NAKANO, T.; TOMINAGA, J.; ARAI, T. The size control of silver nano-particles in SiO₂ matrix film. **Nanotechnology**, v. 16, p. 1565–1568, 2005.

LATEEF, A.; AZEEZ, M. A.; ASAFA, T. B.; et al. Biogenic synthesis of silver nanoparticles using a pod extract of *Cola nitida*: Antibacterial and antioxidant activities and application as a paint additive. **Integrative Medicine Research**, v. 10, n. 4, p. 551–562, 2016. Taibah University. Disponível em: <<http://dx.doi.org/10.1016/j.jtusci.2015.10.010>>. .

LI, M. F.; SUN, S. N.; XU, F.; SUN, R. C. Formic acid based organosolv pulping of bamboo (*Phyllostachys acuta*): Comparative characterization of the dissolved lignins with milled wood lignin. **Chemical Engineering Journal**, v. 179, p. 80–89, 2012. Elsevier B.V. Disponível em: <<http://dx.doi.org/10.1016/j.cej.2011.10.060>>. .

LIU, J.; SONSHINE, D. A.; SHERVANI, S.; HURT, R. H. Controlled Release of Biologically Active Silver from Nanosilver surfaces. **ACS Nano**, v. 4, n. 11, p. 6903–6913, 2010.

LOKINA, S.; STEPHEN, A.; KAVIYARASAN, V.; ARULVASU, C.; NARAYANAN, V. Cytotoxicity and antimicrobial activities of green synthesized silver nanoparticles. **European Journal of Medicinal Chemistry**, v. 76, p. 256–263, 2014. Elsevier Ltd. Disponível em: <<http://dx.doi.org/10.1016/j.ejmech.2014.02.010>>. .

MANIKPRABHU, D.; LINGAPPA, K. Synthesis of silver nanoparticles using the *Streptomyces coelicolor* klmp33 pigment: An antimicrobial agent against extended-spectrum beta-lactamase (ESBL) producing *Escherichia coli*. **Materials Science and Engineering C**, v. 45, p. 434–437, 2014. Elsevier B.V. Disponível em: <<http://dx.doi.org/10.1016/j.msec.2014.09.034>>. .

MILCZAREK, G.; REBIS, T.; FABIANSKA, J. One-step synthesis of lignosulfonate-stabilized silver nanoparticles. **Colloids and Surfaces B: Biointerfaces**, v. 105, p. 335–341, 2013. Elsevier B.V. Disponível em: <<http://dx.doi.org/10.1016/j.colsurfb.2013.01.010>>. .

MOHAN, S.; OLUWAFEMI, O. S.; GEORGE, S. C.; et al. Completely green synthesis of dextrose reduced silver nanoparticles, its antimicrobial and sensing properties. **Carbohydrate Polymers**, v. 106, n. 1, p. 469–474, 2014. Elsevier Ltd. Disponível em: <<http://dx.doi.org/10.1016/j.carbpol.2014.01.008>>. .

NANDA, A.; SARAVANAN, M. Biosynthesis of silver nanoparticles from *Staphylococcus aureus* and its antimicrobial activity against MRSA and MRSE. **Nanomedicine: Nanotechnology, Biology, and Medicine**, v. 5, n. 4, p. 452–456, 2009. Elsevier B.V. Disponível em: <<http://dx.doi.org/10.1016/j.nano.2009.01.012>>. .

NARAYANAN, K. B.; SAKTHIVEL, N. Extracellular synthesis of silver nanoparticles using the leaf extract of *Coleus amboinicus* Lour. **Materials Research Bulletin**, v. 46, n. 10, p. 1708–1713, 2011. Elsevier Ltd. Disponível em: <<http://dx.doi.org/10.1016/j.materresbull.2011.05.041>>. .

NEL, A. E.; MÄDLER, L.; VELEGOL, D.; et al. Understanding

biophysicochemical interactions at the nano–bio interface. **Nature - Materials**, v. 8, n. 7, p. 543–557, 2009. Nature Publishing Group. Disponível em: <<http://dx.doi.org/10.1038/nmat2442>>. .

OBST, J. R. Guaiacyl and syringyl lignin composition in hardwood cell components. **Holzforschung**, v. 36, n. 3, p. 143–152, 1982.

PRATHNA, T. C.; CHANDRASEKARAN, N.; RAICHUR, A. M.; MUKHERJEE, A. Biomimetic synthesis of silver nanoparticles by Citrus limon (lemon) aqueous extract and theoretical prediction of particle size. **Colloids and Surfaces B: Biointerfaces**, v. 82, n. 1, p. 152–159, 2011. Elsevier B.V. Disponível em: <<http://dx.doi.org/10.1016/j.colsurfb.2010.08.036>>. .

PROW, T. W.; GRICE, J. E.; LIN, L. L.; et al. Nanoparticles and microparticles for skin drug delivery. **Advanced Drug Delivery Reviews**, v. 63, n. 6, p. 470–491, 2011. Elsevier B.V. Disponível em: <<http://dx.doi.org/10.1016/j.addr.2011.01.012>>. .

RAO, N. H.; N, L.; PAMMI, S. V; et al. Green synthesis of silver nanoparticles using methanolic root extracts of Diospyros paniculata and their antimicrobial activities. **Mater Sci Eng C Mater Biol Appl**, v. 62, p. 553–557, 2016. Elsevier B.V. Disponível em: <<http://www.ncbi.nlm.nih.gov/pubmed/26952458>%5Cnhttp://ac.els-cdn.com/S0928493116300716/1-s2.0-S0928493116300716-main.pdf?_tid=94d79c70-f0c7-11e5-bc74-00000aacb362&acdnat=1458717749_4c3ea9b5783ecd666f675bb3e8007f4e>. .

RAVINDRAN, A.; CHANDRAN, P.; KHAN, S. S. Biofunctionalized silver nanoparticles: Advances and prospects. **Colloids and Surfaces B: Biointerfaces**, v. 105, p. 342–352, 2013. Elsevier B.V. Disponível em: <<http://dx.doi.org/10.1016/j.colsurfb.2012.07.036>>. .

RENCORET, J.; MARQUES, G.; GUTIÉRREZ, A.; et al. Isolation and structural characterization of the milled-wood lignin from Paulownia fortunei wood. **Industrial Crops and Products**, v. 30, n. 1, p. 137–143, 2009.

RICHTER, A. P.; BROWN, J. S.; BHARTI, B.; et al. An environmentally benign antimicrobial nanoparticle based on a silver-infused lignin core. **Nature Nanotechnology**, v. 10, n. 9, p. 817–823, 2015. Nature Publishing Group. Disponível em: <<http://www.nature.com/doi/10.1038/nnano.2015.141>>. .

SANGHI, R.; VERMA, P. Biomimetic synthesis and characterisation of protein capped silver nanoparticles. **Bioresource Technology**, v. 100, n. 1, p. 501–504, 2009.

SANKAR, R.; KARTHIK, A.; PRABU, A.; et al. Origanum vulgare mediated biosynthesis of silver nanoparticles for its antibacterial and anticancer activity. **Colloids and Surfaces B: Biointerfaces**, v. 108, p. 80–84, 2013. Elsevier B.V. Disponível em: <<http://dx.doi.org/10.1016/j.colsurfb.2013.02.033>>. .

SARAVANAKUMAR, A.; GANESH, M.; JAYAPRAKASH, J.; JANG, H. T. Biosynthesis of silver nanoparticles using Cassia tora leaf extract and its antioxidant and antibacterial activities. **Journal of Industrial and Engineering Chemistry**, v. 28, p. 277–281, 2015. The Korean Society of Industrial and Engineering Chemistry. Disponível em: <<http://dx.doi.org/10.1016/j.jiec.2015.03.003>>. .

SCHMETZ, Q.; MANIET, G.; JACQUET, N.; et al. Comprehension of an organosolv process for lignin extraction on Festuca arundinacea and monitoring of

the cellulose degradation. **Industrial Crops & Products**, v. 94, p. 308–317, 2016. Elsevier B.V. Disponível em: <<http://dx.doi.org/10.1016/j.indcrop.2016.09.003>>. .

SHEN, Z.; HAN, G.; LIU, C.; WANG, X.; SUN, R. Green synthesis of silver nanoparticles with bagasse for colorimetric detection of cysteine in serum samples. **Journal of Alloys and Compounds**, v. 686, p. 82–89, 2016. Elsevier Ltd. Disponível em: <<http://dx.doi.org/10.1016/j.jallcom.2016.05.348>>. .

SINGH, P.; KIM, Y. J.; ZHANG, D.; YANG, D. C. Biological Synthesis of Nanoparticles from Plants and Microorganisms. **Trends in Biotechnology**, v. 34, n. 7, p. 588–599, 2016. Elsevier Ltd. Disponível em: <<http://dx.doi.org/10.1016/j.tibtech.2016.02.006>>. .

SINGH, S. K.; DHEPE, P. L. Isolation of lignin by organosolv process from different varieties of rice husk: Understanding their physical and chemical properties Lignin producing processes. **Bioresource Technology**, v. 221, p. 310–317, 2016. Elsevier Ltd. Disponível em: <<http://dx.doi.org/10.1016/j.biortech.2016.09.042>>. .

SRIRANJANI, R.; SRINITHYA, B.; VELLINGIRI, V.; et al. Silver nanoparticle synthesis using Clerodendrum phlomidis leaf extract and preliminary investigation of its antioxidant and anticancer activities. **Journal of Molecular Liquids**, v. 220, p. 926–930, 2016. Elsevier B.V. Disponível em: <<http://dx.doi.org/10.1016/j.molliq.2016.05.042>>. .

SUMAN, T. Y.; RADHIKA RAJASREE, S. R.; KANCHANA, A.; ELIZABETH, S. B. Biosynthesis, characterization and cytotoxic effect of plant mediated silver nanoparticles using Morinda citrifolia root extract. **Colloids and Surfaces B: Biointerfaces**, v. 106, p. 74–78, 2013. Elsevier B.V. Disponível em: <<http://dx.doi.org/10.1016/j.colsurfb.2013.01.037>>. .

SUN, Q.; CAI, X.; LI, J.; et al. Green synthesis of silver nanoparticles using tea leaf extract and evaluation of their stability and antibacterial activity. **Colloids and Surfaces A: Physicochemical and Engineering Aspects**, v. 444, p. 226–231, 2014. Elsevier B.V. Disponível em: <<http://dx.doi.org/10.1016/j.colsurfa.2013.12.065>>. .

TAGAD, C. K.; DUGASANI, S. R.; AIYER, R.; et al. Green synthesis of silver nanoparticles and their application for the development of optical fiber based hydrogen peroxide sensor. **Sensors and Actuators, B: Chemical**, v. 183, p. 144–149, 2013. Elsevier B.V. Disponível em: <<http://dx.doi.org/10.1016/j.snb.2013.03.106>>. .

TEJADO, A.; PEÑA, C.; LABIDI, J.; ECHEVERRIA, J. M.; MONDRAGON, I. Physico-chemical characterization of lignins from different sources for use in phenol-formaldehyde resin synthesis. **Bioresource Technology**, v. 98, p. 1655–1663, 2007.

TOLEDANO, A.; GARCÍA, A.; MONDRAGON, I.; LABIDI, J. Lignin separation and fractionation by ultrafiltration. **Separation and Purification Technology**, v. 71, n. 1, p. 38–43, 2010.

TOLEDANO, A.; SERRANO, L.; GARCIA, A.; MONDRAGON, I.; LABIDI, J. Comparative study of lignin fractionation by ultrafiltration and selective precipitation. **Chemical Engineering Journal**, v. 157, n. 1, p. 93–99, 2010.

VALODKAR, M.; JADEJA, R. N.; THOUNAOJAM, M. C.; DEVKAR, R. V.; THAKORE, S. In vitro toxicity study of plant latex capped silver nanoparticles in

human lung carcinoma cells. **Materials Science and Engineering C**, v. 31, n. 8, p. 1723–1728, 2011. Elsevier B.V. Disponível em: <<http://dx.doi.org/10.1016/j.msec.2011.08.001>>. .

VILAS, V.; PHILIP, D.; MATHEW, J. Essential oil mediated synthesis of silver nanocrystals for environmental, anti-microbial and antioxidant applications. **Materials Science and Engineering C**, v. 61, p. 429–436, 2016. Elsevier B.V. Disponível em: <<http://dx.doi.org/10.1016/j.msec.2015.12.083>>. .

WANG, F.; TANG, S.; YU, Y.; et al. Preparation of palladium nanoparticle catalyst in ionic liquid and its catalytic properties for Heck-Mizoroki reaction. **Cuihua Xuebao/Chinese Journal of Catalysis**, 2014.

WANI, I. A.; KHATOON, S.; GANGULY, A.; AHMED, J.; AHMAD, T. Structural characterization and antimicrobial properties of silver nanoparticles prepared by inverse microemulsion method. **Colloids and Surfaces B: Biointerfaces**, v. 101, p. 243–250, 2013. Elsevier B.V. Disponível em: <<http://dx.doi.org/10.1016/j.colsurfb.2012.07.001>>. .

WEI, L.; LU, J.; XU, H.; et al. Silver nanoparticles: Synthesis, properties, and therapeutic applications. **Drug Discovery Today**, v. 20, n. 5, p. 595–601, 2015. Elsevier Ltd. Disponível em: <<http://dx.doi.org/10.1016/j.drudis.2014.11.014>>. .

WWW.INDEXMUNDI.COM.
<http://www.indexmundi.com/agriculture/?commodity=palm-oil>. .

ZHANG, Y.; CHENG, X.; ZHANG, Y.; XUE, X.; FU, Y. Biosynthesis of silver nanoparticles at room temperature using aqueous aloe leaf extract and antibacterial properties. **Colloids and Surfaces A: Physicochemical and Engineering Aspects**, v. 423, p. 63–68, 2013. Elsevier B.V. Disponível em: <<http://dx.doi.org/10.1016/j.colsurfa.2013.01.059>>.